University of Southampton Research Repository

University of Southampton

Improvement of printable organic based thermoelectric materials

MPhil Thesis

By

Jake Lawrie-Ashton

Supervisors:

Professor Steve Beeby

Dr Iris Nandhakumar

Professor Richard Whitby

Contents

List of abbreviations

PEDOT	Poly(3,4-ethylenedioxythiophene)
PEDOT-MeOH	Poly(hydroxy-methylated-3,4-ethylenedioxythiophene)
PProDOT	Poly(3,4-propylenedioxythiophene)
PSS	Polystyrene sulphonate
Tos	Tosylate
EDOT	3,4-Ethylenedioxythiophene
DMSO	Dimethyl sulfoxide
DLS	Dynamic light scattering
DI	Deionised
MAI	Methyl ammonium iodine
DMF	Dimethylformamide
EG	Ethylene glycol
XPS	X-ray photoelectron spectroscopy
TDAE	Tetrakis(dimethylamino)ethylene
UV-Vis-NIR	ultraviolet–visible-near-infrared spectrophotometry
SDS	Sodium dodecyl sulphonate

Chapter 1 Introduction

1.1   Motivation and objectives

Energy use is currently higher than ever and estimations suggest that it will keep rising.[1] This demand of energy can put stress on the natural resources available to us. Waste energy harvesting is a method to contribute towards meeting these energy demands. Most waste energy is in the form of heat, and as thermoelectric generators turn this heat into usable electricity they can be an option for collecting this energy.[2]

Organic based thermoelectric devices can offer a good alternative to their inorganic counterparts in low temperature applications. They comparatively have a lower cost, fewer environmental effects and are in higher abundance.

Increasing the thermoelectric figure of merit (ZT) for P-type polymers will assist in the commercialisation of organic based thermoelectric devices, as currently the output power is too low for most consumer electronics. The target is to increase the room temperature ZT to near 1, and therefore near the same scale as inorganic materials such as Bismuth Chalcogenides so that polymers may start to be used in place of inorganic materials. Formulating these materials such that it is possible to print devices from them and that they remain flexible allows increased possibilities for their application such as for integrated fabric technology.

Currently the bulk of research into organic based thermoelectric materials has focused on poly(3,4-ethylenedioxythiophene) (PEDOT). This is a commercially available material. However the commercially available formulations are not designed to enhance thermoelectric properties. Furthermore the exact contents of the product is often not disclosed. It is unclear how other additives already in the mix affect the thermoelectric properties, these additives such as DMSO and various glycols can change the physical structure of the printed material and the in some cases the orbital energy levels causing changes in the reduction level of the polymers.[13] PEDOT is readily synthesisable in laboratory condition. By polymerising in the lab greater control can be taken and the effect of every additive on material properties can be seen. The properties of interest include, but are not limited to, film quality, electrical conductivity, thermal conductivity and Seebeck coefficient.

PEDOT has many derivatives such as poly(hydroxy- methylated-3,4-ethylenedioxythiophene) (PEDOT-MeOH) or poly(3,4-propylenedioxythiophene) (PProDOT). These P-type conducting polymers are unexplored with respect to thermoelectric properties, this is due to current commercial availability. These could offer a more efficient alternative to PEDOT for thermoelectric polymers.

The Main Aims and objectives are as follows:

•   Investigate whether high quality PEDOT:PSS films can be made with minimal dopant except a small ratio, up to 10 %, of DMSO

•   Determine the electrical conductivity and Seebeck coefficient of these films

•   Investigate the effect of dopants/additives such as ethylene glycol and DMSO on PEDOT:PSS with respect to print quality, electrical conductivity and Seebeck coefficient

•   Investigate PEDOT derivatives and how their properties differ from PEDOT:PSS

•   Print a device using lab made PEDOT:PSS or derivative

1.2   Background theory

Thermoelectric generators convert a temperature difference into a potential, based on the Seebeck effect.[3] They are often made of semiconductor materials and work by thermally promoting electrons to increase charge carrier concentration at the hot side. In a p-type the positive charge carriers (holes) will then flow from the hot side to the cold side and in a n-type the electrons will flow from hot to cold. This is shown in figure 1, a thermoelectric generator will be made of many of these cells which are thermally in parallel but electrically in series. This current produces a voltage, which is called the Seebeck voltage. The system will work in reverse too using the Peltier effect where a current is applied across the material and a thermal gradient is formed.[3] By using only a single couple the current produced is generally far too low for any practical use, thus there are often many of these p-n junctions connected thermally in parallel.
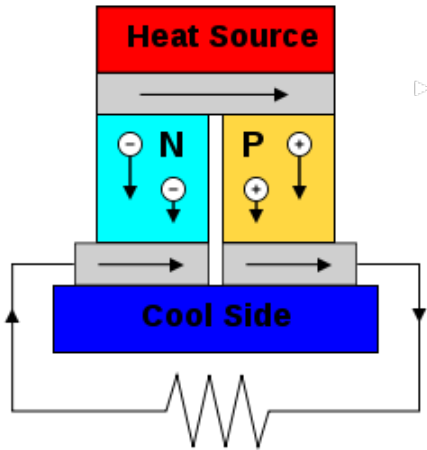
Equation 1 shows the Seebeck effect mathematically.

Equation 1
$$S = \frac{V}{\Delta T}$$

Where S is the Seebeck coefficient in V K^{-1}, V is the potential produced by the thermal gradient in V and ΔT is the temperature difference in K.

S is just one property of a thermoelectric material, using this to compare the thermoelectric properties of materials would be redundant as there are many other factors that contribute to performance. The thermoelectric figure of merit is denoted as ZT shown in equation 2, this allows direct comparison between material. The ZT is a measure of how efficiently a material can convert heat energy into usable electricity.

Equation 2
$$ZT = \frac{S^2 \sigma T}{\kappa}$$

Where σ is the electrical conductivity in $S\ m^{-1}$, κ is the thermal conductivity in $W\ m^{-1}\ K^{-1}$, T is the mean temperature of the system in K, S is the Seebeck coefficient in $V\ K^{-1}$ and κ is the thermal conductivity which is comprised of an electrical component, κ_e and a "lattice component" κ_l. κ_e is controlled by the flow of electrons in the material and κ_L is governed by the material structure. It is shown from this that to achieve an improvement in a thermoelectric material it is key to either increase the Seebeck coefficient or electrical conductivity and lower the thermal conductivity. $S^2\sigma$ is often referred to as the power factor as this shows the amount of power that can be output in W m^{-1} K^{-1}. Equation 3 shows the

Wiedemann-Franz law. This shows the relationship between electrical and thermal conductivity.

Equation 3
$$\kappa_e = LT\sigma$$

Where κ_e is the electrical component of the thermal conductivity in $\mathrm{W\,m^{-1}\,K^{-1}}$, L is the Lorenz number in $\mathrm{W\,\Omega\,K^{-2}}$, T is the absolute temperature in K and σ is the electrical conductivity in $\mathrm{S\,m^{-1}}$. The Lorenz number is specific for the material type. It is said to be roughly constant for all metals and is reduced in semiconductors.[5] This shows that the electronic component of thermal conductivity is directly proportional to the electrical conductivity of that conductive material , so any improvement in electrical conductivity is combatted by an increase in the thermal conductivity, which will lower the thermal gradient. This effect however is most relevant in metals, where the main form of thermal conductivity is from electronic factors, whereas in inorganic semiconductors the main form of thermal conductivity tends to be derived from thermal conduction through the lattice in the form of vibrations and defects.[6] This effect has not been greatly studied within organic semiconductors. However it is clear that there will be a large variance depending on material structure and isotropy. These can be very different based on simple experimental steps like processing methods.[7]

There are a lot of interests in flexible thermoelectric materials, for instance waste heat collection from body heat.[8-10] There has been some progress in flexible thermoelectric materials, however, these have mainly focused on inorganic materials such as Bi_2Te_3 with Sb_2Te_3 imbedded within polymers.[9] These materials generally have a much higher efficiency and therefore thermoelectric figure of merit, although this efficiency is at higher temperatures, than that of organic polymers, predominantly PEDOT, PEDOT:PSS (PEDOT:Polystyrene sulphonate) and PEDOT:Tos (PEDOT:Tosylate) However a major drawback of these inorganic materials is that they also come with greater safety risks due to the use of heavy metals, they are also mainly inflexible and require high temperatures in processing .[8, 11] Heavy metals also have relatively low abundance in the earth, especially in comparison to carbon. Figure 2 shows the structures of, PEDOT, PSS and Tos
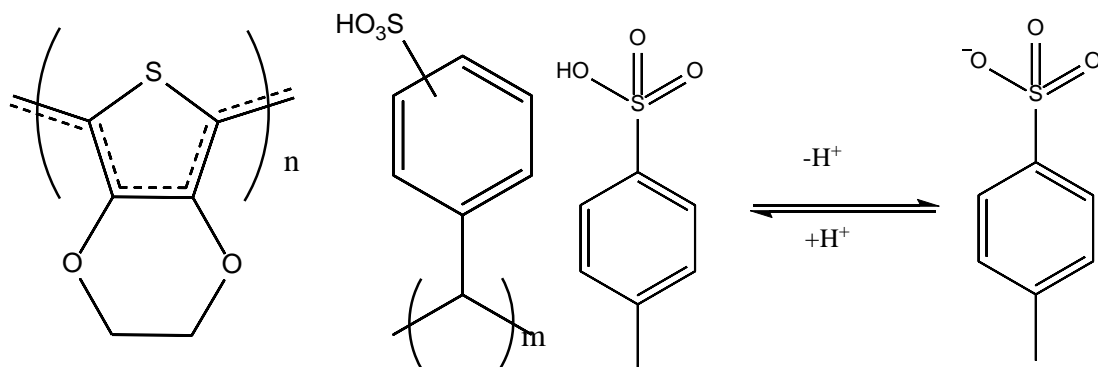
Figure 2 PEDOT (left), PSS (middle), Tos (right pair)

Processing methods can have an effect on the isotropy and morphology of the material, many organic thermoelectric samples are produced via spin coating.[12-14] In this approach a viscous solution is slowly poured onto a substrate that is then spun at a high rate, such as 1000 RPM. It is believed that the spinning can cause the orientation of the molecules within the structures to be such that conductivity is different in the direction between the centre of the sample and the outer edge as opposed to perpendicular to this plane. With PEDOT:PSS this anisotropy has been shown to be between 1.4 and 1.6.[6, 15] Printed samples have been shown to be more random with regards to molecular orientation so measurements are more consistent and have a much lower dependency on sample orientation.[7]

There are 3 main methods in which devices can be printed: screen printing, dispenser printing and inkjet printing.[16] Inkjet printing is achieved by forcing an ink reservoir to drop ink at a set rate. A portion of these drops are then ionised. These ionised droplets are then deflected from a charged plate and fall onto the sample. The droplets which are not ionised fall straight and are caught and recycled by a gutter. Depending on the dropping mechanism, thermal or piezo-driven, there are different ink requirements, such as boiling point, viscosity and surface tension.[17] Often low viscosity inks are necessary to achieve proper printing, however, this can cause overly thin thermoelectric layers so multiple layers may have to be printed. [18]

Screen printing is achieved by depositing an ink through a porous mesh that has a photolithographically patterned emulsion layer that defines the desired printed pattern. Thus, adapting and changing designs can take longer and be more expensive than direct printing methods (e.g. inkjet). To print, a flexible rubber blade (squeegee) is lowered onto the screen which has the ink smeared evenly across its surface. The squeegee is then passed across the template pushing the ink through the exposed mesh onto the substrate. Unlike

inkjet printing, thicker films are relatively easy to achieve through the use of viscous inks and suitable screen properties (mesh characteristics and emulsion thickness). Thicker films will require longer annealing times which can add to processing cost.[9, 19, 20] One other limitation with screen printing is that when volatile solvents are used in the ink it's composition can change during extended printing runs. This is because unlike inkjet and dispenser printing the ink is used in a situation with a high surface area to volume ratio causing much higher evaporation rates, an issue that becomes more relevant during up-scaling of experiments or commercial implementation.[19]

Dispenser printing is in theory the most versatile of the 3 allowing the design capabilities of ink jet printing with the choice of almost any ink.[21] In dispenser printing a syringe is filled with the desired ink, which is then attached to a vacuum line where a negative pressure is set. This is necessary to hold the ink in the syringe so that it does not flow due to gravity. Then a positive pressure can be applied through the same line for a set period of time allowing a set volume to be dispensed. This can be done on a drop by drop basis or continuously. Automated x-y-z micro positioners enable full control of where the syringe dispenses and designs can quickly be achieved.[22] An issue with this method is getting the initial settings right can be difficult and lengthy. Dependant on the viscosity and particle size within the ink different dispenser tips can be used, but again different tips for the same ink need different settings. Ensuring that the ink behaves as a Newtonian liquid can be a problem when high concentrations of substrate are used.[18]

1.3   Synthesis

Much research focus is on adaptation of commercially available PEDOT:PSS, however these are not purely designed for thermoelectric applications. In this research there was a focus on ground up synthesis and design of PEDOT:PSS solutions directly made with the thermoelectric properties in mind.

Oxidative polymerisation of 3,4-Ethylenedioxythiophene (EDOT) in the presence of PSS is a well-known synthesis method and the method employed here.[23] PSS must be used in the polymerisation solution due to the low solubility of PEDOT in water, as the EDOT polymerises it is encapsulated in PSS. It has been shown to be difficult to re-dissolve PEDOT once it has precipitated out of solution. [24]

The initial synthesis uses $Na_2S_2O_8$ as an oxidising agent. During the polymerisation this is converted into Na_2SO_4, an ionic species. To remove this impurity from the reaction mixture ion exchange resins were used. Amberlite IR 120, H form and Ambersep 900, OH form, were chosen for this purpose as one will exchange for H^+ ions and one for OH^- ions leaving water instead of Na_2SO_4.

Figure 3 shows the reaction scheme for the synthesis. [23,24] The oxidative polymerisation leaves PEDOT with a 2+ charge per 6 monomers, this however is an average. This is then charge balanced by a deprotonated sulphonic acid group on PSS.
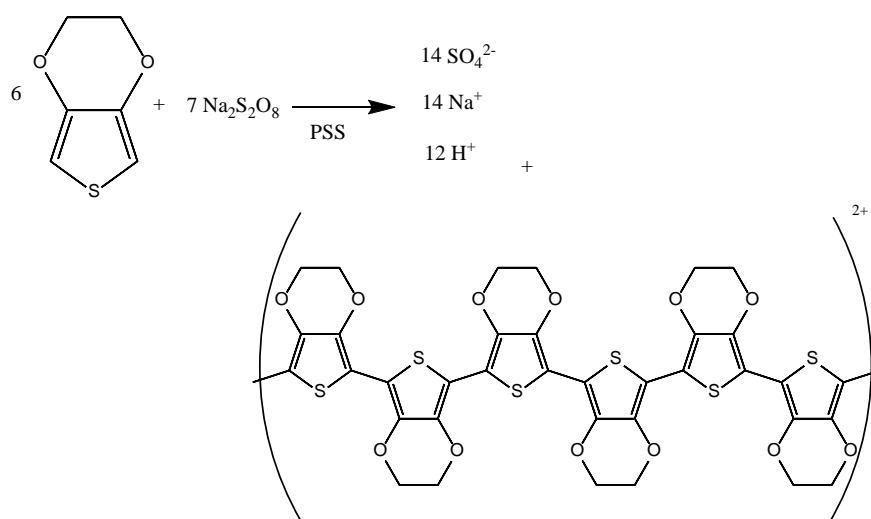
Figure 3 Reaction scheme for the oxidative polymerisation of EDOT to PEDOT

Chapter 2 Literature Review

2.1   Introduction

In this section the state of the art with respect to thermoelectric materials, applications and processing methods will be highlighted and critically reviewed. There will be a focus on those appropriate for flexible, wearable devices and PEDOT.

2.2   Applications

Wearable thermoelectric devices have been produced, although they currently generally come in crude, inflexible and made in small scale methods such as adapting available clothing with all the necessary devices and wires. Devices tend to focus on warmer areas of the body, such as the wrist and head. These are both also particularly good locations for thermoelectric devices to be worn as they tend to allow more air flow than other warm parts, such as chest.[25, 26]

The use of thermoelectric devices in a wearable application has been explored by attaching commercially available rigid thermoelectric generators to clothing.[25-27] Devices implanted into shirts have produced up to 50 μW cm^{-2} while cycling.[26] It was found that one of the main factors to power output is based upon the ability to keep the cold side of the device cold. To achieve this on a shirt a carbon fabric heat-spreading layer has been used to wick away the heat. This was found more efficient than having the outer layer of the device open to air.[26] It is deemed to be a "reliable power source for low-power wearable electronics such as health monitoring devices"[26]. There are 2 main draw backs to this device, to start the cost is 10 X higher than just using batteries for the same purpose. Secondly, the devices being used are inflexible, although it is stated that the clothing is still comfortable it limits the usable area of the shirt. If flexible devices were instead used and integrated into the fabric a significantly larger portion of the clothing could be used, thus amount of energy harvested could increase.

Aside from clothing integrated devices, commercial thermoelectric generators have been adapted for use in medical applications where the device is fitted on the head or wrist. While these devices may be appropriate for the use, the devices would be difficult to be used on mass due to comfort among other social limitations.[28] These devices also use heavy metals and thus introduce a large cost and environmental issues as mentioned previously.

Use of PEDOT:PSS lends itself greatly to wearable technology as it is inherently flexible and safe. It is also very adaptable within processing capabilities.[29] It is comparably light and although exhibits a low ZT can be used in a larger area due to its properties. PEDOT:PSS has also been shown to be capable of coating polyester fabric while retaining many of the fabrics properties. [29] This fabric can then be used to produce clothing generally, although there are some issues with this, as the thermoelectric material is applied in a planar manner there will be limited locations in which it can be used. To treat the polyester it is simply soaked and sonicated in a dimethyl sulfoxide (DMSO)/PEDOT:PSS solution for 2 h and then dried at 130 ^{o}C for 15 min.[29]

There has been progress in bespoke devices for biometric sensors, a prototype consisted of thin films of p-Sb_2Te_2 and n-Bi_2Te_3 sputtered onto Kapton.[30] The planar device was made of

100 thermocouples and produced 430 mV with a power of 32 nW at 40 K temperature difference. This is higher than would be expected for a wearable device, but output values are on the scale necessary for biometric sensors. The deposited thin films were 500 nm thick, and were deposited on 50 μm Kapton. In reality the device would have to be made of 734 thermocouples to get the required power at a thermal gradient of 10 K. The device, although made for harvesting energy from human body heat is not on a wearable sample. Figure 4 shows the device on Kapton.
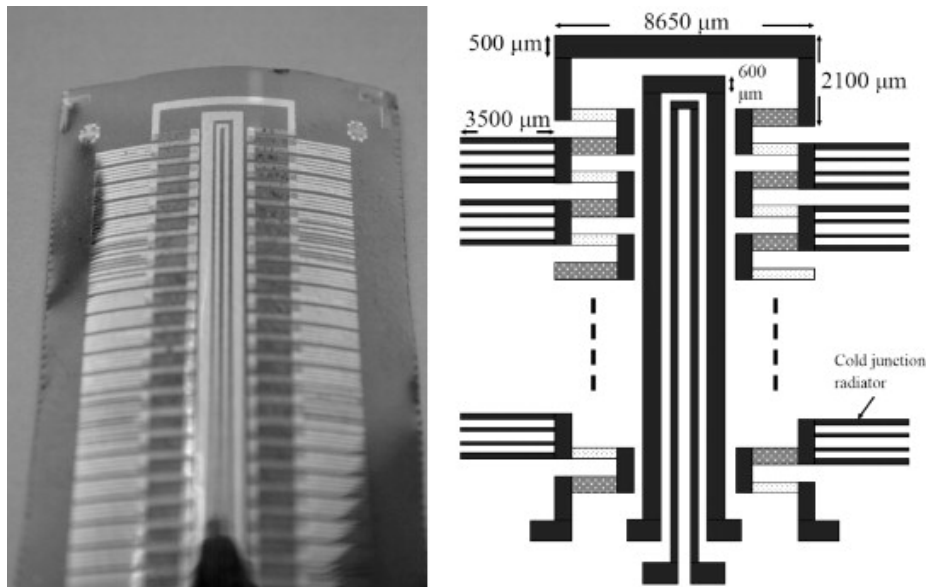

Figure 4 Left, photograph of flexible thermoelectric device on Kapton, right schematic of flexible thermoelectric generator, reproduced from reference [30]

2.3   Materials

Organic polymers have the potential for safe and flexible thermoelectric materials, however currently have poor performance. Table 1 shows the currently highest figures of merits available.

MATERIAL	σ / S cm^{-1}	S / μV K^{-1}	ZT	REF
TELLURIUM NANOWIRE-PEDOT: PSS	334.68		0.390	[31, 32]
PEDOT/GRAPHENE AND PEDOT/ CNTS	208.40		0.031	[32, 33]
PEDOT: PSS-GRAPHENE-TIO2	260.00	−47.00	0.0048	[32, 34]
POLY(VINYL CHLORIDE)-CNTS	629.90	30.50	0.30	[32, 35]
PEDOT:TOS	300	780	0.25	[36]
PEDOT:PSS-DMSO MIXED	940	72	0.48	[6]

Table 1 highlighting the State of the art organic polymer based thermoelectric materials available

Many of the high ZT polymer based thermoelectric materials are based upon PEDOT:PSS with some further form of doping. Many of the additives used such as DMSO, carbon nanotubes and graphene are used to increase the electrical conductivities of the materials.[24] Another crucial point to be made is that the main progress in thermoelectric polymers is based upon p-type materials. N-type polymers for thermoelectric devices are currently a rarity due to low commercial availability, this availability is due to the instability of a negative charge in most organic systems. Many N-Type Polymers are highly reactive towards oxygen so are not stable in air and have a short lifetime.

PEDOT:PSS has been shown to have a grain like structure with PSS being the main component with an estimated molecular weight of 400,000 g mol^{-1}.[37] Entwined in this PSS chain are sections of PEDOT with an approximate molecular weight of 1000-2500 g mol^{-1}. This chain then entangles itself and others, forming in water a globular structure with the hydrophobic PEDOT being fully encompassed by the PSS. This is shown in Figure 5.
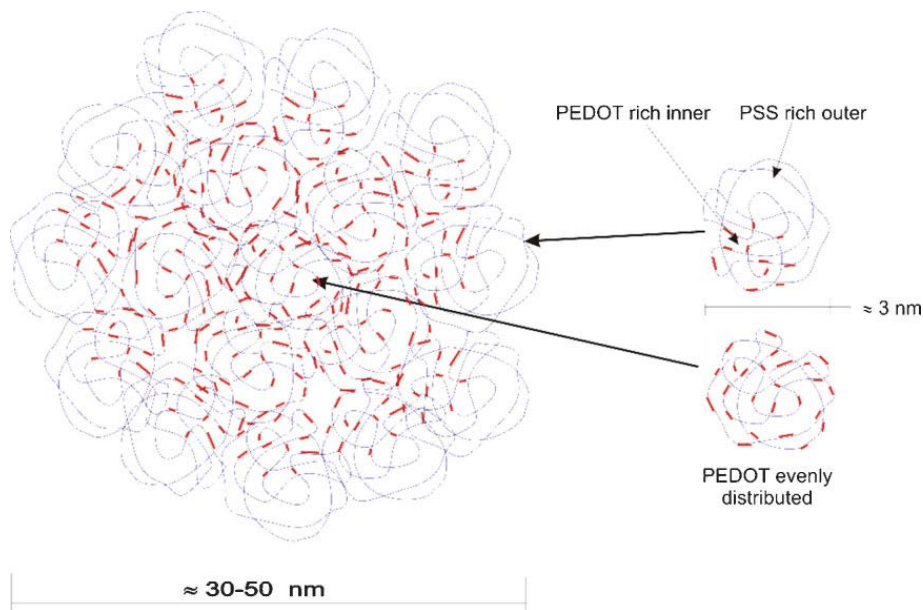
Figure 5 hypothesised PEDOT:PSS grain structure with smaller PEDOT segments encompassed in many longer PSS chains, image reproduced from reference [37]

These grains stack side by side and are connected by hydrogen bonds between the sulphonate groups. The morphology of the film is related to the production method of the device/sample. If spin coating is applied then the grains are shown to be "pancake like" in structure due to the centrifugal force applied to them. If the films are drop casted, they tend to be more "lentil like" in structure with more surface character. Introducing DMSO into a sample is shown to increase the conductivity of the sample by allowing grains to join.[24, 38]

The above mentioned estimated molecular weight of PEDOT can be altered. This is due to the polymeric nature of PEDOT. This difference in chain length can have an impact on the thermoelectric properties.[39] Increasing the chain length has been shown to increase the electrical conductivity and the Seebeck coefficient of post print treated samples. Tables 2 and 3 highlights these post treatments and the effect of chain length can be seen by comparing that of Clevios P and Clevios PH100. These are commercially available inks with two different PEDOT chain lengths, Clevios PH100 being the larger of the both. There are challenges with the conclusions drawn here however. The molecular size of PEDOT from both inks is concluded from Dynamic light scattering (DLS) data on dilute samples of each ink.[39] It is concluded that due to there being larger particles in Clevios PH1000 over that of Clevios P that the PEDOT length is longer. However similar studies of PEDOT:PSS where DLS data has been carried out have attributed the particle sizes calculated to the PEDOT:PSS complex as a

whole, and as described before suggested that the PEDOT in the samples remain in relatively small.[23] This challenge aside it appears that post print treatments improve the thermoelectric properties significantly. These were achieved by adding a droplet of ~ 100 μL onto the substrate and heating it to 140 °C until dry. The samples were then allowed to cool, rinsed with deionised (DI) water and then dried again at 140 °C. The samples from Table 3 were further treated with NaOH after this treatment.

	Seebeck coefficient (μV/K)		electrical conductivity (S/cm)		power factor (μW/(m K^2))	
	Clevios P	CleviosPH1000	Clevios P	Clevios PH1000	Clevios P	Clevios PH1000
untreated			0.3	0.3		
HFA·3H$_2$O-treated	14.5 ± 0.2	24.8 ± 1.0	226 ± 23	1206 ± 20	4.7	74
EG-treated	14.6 ± 0.3	22.6 ± 0.8	211 ± 12	1222 ± 82	4.5	69.2
MAI/DMF-treated	14.7 ± 0.7	22.7 ± 1.4	236 ± 26	2100 ± 112	5.1	108.2
H$_2$SO$_4$-treated^a	12 ± 0.8	16.5 ± 0.7	281 ± 18	2156 ± 92	4.0	58.7
H$_2$SO$_4$-treated^b	10.8 ± 1.1	17.3 ± 1.0	420 ± 36	3088 ± 123	4.9	92.4

^{a}Treated by H$_2$SO$_4$ once. ^{b}Treated by H$_2$SO$_4$ three times.

Table 2 Comparison of TE property of the PEDOT:PSS films (Clevios P and Clevios PH1000) treated with various post-treatments reproduced from reference [39]

	Seebeck coefficient (μV/K)		electrical conductivity (S/cm)		power factor (μW/(m K^2))	
	Clevios P	Clevios PH1000	Clevios P	Clevios PH1000	Clevios P	Clevios PH1000
HFA·3H$_2$O-treated	16.5 ± 1.7	28.5 ± 2.9	203 ± 27	995 ± 99	5.5	80.8
EG-treated	17.1 ± 1.5	34.5 ± 2.4	174 ± 4	966 ± 43	5.1	115.0
MAI/DMF-treated	18.8 ± 1.9	28.5 ± 2.2	176 ± 18	1550 ± 155	6.2	125.9
H$_2$SO$_4$-treated^a	19.2 ± 1.9	38.1 ± 0.6	229 ± 32	1178 ± 118	8.4	171.0
H$_2$SO$_4$-treated^b	19.5 ± 2.0	37.1 ± 2.9	299 ± 18	2170 ± 201	11.4	334.0

^{a}Treated by H$_2$SO$_4$ once. ^{b}Treated by H$_2$SO$_4$ three times.

Table 3 Comparison of TE property of the PEDOT:PSS films (Clevios P and Clevios PH1000) treated with various post-treatments and further base treatment [39]

The largest power factor in tables 2 and 3 without further base treatment is Methyl ammonium iodine/ dimethylformamide (MAI/DMF)-treated. This use of MAI with solvents and co-solvents was investigated further. Treatment with MAI allowed significantly better properties than without and the use of co-solvents has been shown to be much more effective than using just organic solvents. The suggested mechanism for this improvement comes in two parts, first the de-doping of PSS by selective dissolution. Secondly a conformational change in PEDOT from a coiled to an extended coil or linear confirmation. This was observed by atomic force microscopy showing clear nanosized fibrous structures. [39]

Within studies of PEDOT:PSS there has been a large improvement over recent years with currently the highest ZT published to be 0.42.[6] This figure was achieved by using PEDOT:PSS, spin coated onto glass for electrical measurements and pipetted onto SiO$_2$ for thermal

measurements. This high thermoelectric figure of merit was achieved by de-doping of PSS to change the free the carrier concentration, conductivity and therefore Seebeck coefficient. Initially a PEDOT:PSS 1:2.5 (mass ratio) solution was mixed with 5 vol % ethylene glycol (EG) or DMSO and then spin coated onto the samples. The de-doping was then achieved by selective dissolution of PSS using 5 vol% EG at 60 $^{\circ}$C or room temperature for DMSO. The de-doping was performed for varying lengths of time. X-ray photoelectron spectroscopy (XPS), Seebeck coefficient, thermal conductivity and electrical conductivity measured at every 10 minutes, up to 150 minutes. The de-doping occurs due to the PSS being hydrophilic and PEDOT being hydrophobic, thus in a polar organic solvent, such as EG, PSS will solvate where PEDOT will not. Due to the intermolecular forces and internal structure of dry PEDOT:PSS the solvation of PSS will slow as the ratio of the two tend towards 1. As the PEDOT and PSS are only bound together by ionic interactions it is relatively easy for EG to displace the PEDOT. Once the PEDOT has been displaced it will likely find another PSS molecule to bind to, further saturating the PSS, increases the difficulty of dissolution. This was measured in this case by using XPS. In this technique the intensity of the S(2p) peaks was measured with time, as sulphur is present in both PEDOT and PSS. As PSS is solvated the relative intensity of the peak corresponding to PSS decreased until 60 minutes at which point it stayed consistent with PEDOT. This shows the selective dissolution. As well as the above mentioned measurements, thickness was measured during the experiment; within this first hour period the thickness of the samples dropped dramatically by over half in some cases. After this time there was little to no change in the thickness of the samples, showing that dissolution had completed.

During this dissolution the Seebeck coefficient is shown to increase over the first 100 minutes and then plateau with the main changes occurring during the first hour with de-doping. It is thought that this effect is due to an increase in carrier mobility caused by a lower tunnelling distance between PEDOT molecules and saturation of the PSS.[6]

An important point to make here with regards to PEDOT:PSS is that in this de-doping process, or generally considering the ratio of the two, there is not the normal trade-off between thermal conductivity (κ) and electrical conductivity (σ). This is a crucial finding here as this trade of is often what limits the improvement of inorganic thermoelectric materials. This is not the case here due to the material structure, in that the thermal energy is transferred easier with higher portions of PSS. It is supposed that this is due to PSS molecules being larger

and more covalent in character, thus removing the PSS increases the Van der Waals character.[6] This however can be expanded by considering the grain like structure explained above.

The figure of merit expressed above has however been contested. This is largely related to the uncertainty and difficulty in measuring thermal conductivity in polymers as well as the anisotropy in many of the samples made.[15] This has been shown to be up to 3 orders of magnitude of different between highly conducting sections and poorly conducting sections. [7] It was shown using PEDOT:Tos and PEDOT:PSS their thermal and electrical conductivity were proportional to the point that the effect was larger than that predicted by only using the Wiedemann-Franz law. However there are some large differences in how the experiments where conducted. Unlike before the measurements for thermal conductivity, electrical conductivity and Seebeck coefficient were all performed on the same sample. However the samples were produced in a different manner than before, either by vacuum vapour phase polymerisation or chemical polymerisation as opposed to spin coating or pipetting a commercial PEDOT:PSS sample. This can cause vast differences in the samples.[15] Further to this the PEDOT:PSS was not de-doped so the change in thermal conductivity across different dopant levels was not observed. The morphology in these lab scale polymerised samples are unknown such that thermal properties could be identical or vastly different. I would say that these two different results shown are not mutually exclusive due to the many differences present, however, it does show how little is known about transport properties within organic polymers and how processing conditions effect this.

Another technique that has been used to improve the thermoelectric properties of PEDOT is changing the oxidation level.[36] This was achieved by inkjet printing a solution of EDOT, $Fe(Tos)_3$ and pyridine onto a warm (35 ^oC) Au sample. Upon contact with the sample EDOT polymerisation occurs. This synthesis forms PEDOT:Tos. Within this structure, PEDOT has formal positive charges spread through a conjugated pi system and Tos has formal negatives to charge balance, this ionic attraction is what keeps these molecules together. By treating these samples with a reducing agent, tetrakis(dimethylamino)ethylene (TDAE), these positive charges can be changed into neutral chains, which changes the amount of charge carriers within the structure. By reducing the chain the charge balancing Tos is no longer needed and thus will join with the $TDAE^{2+}$ and be dissolved off. As PEDOT and the Tos ions both contain

sulphur in two distinct chemical environments they will exhibit different binding energies in XPS. Thus by looking at the change in ratio of the S(2p) peaks oxidation level can be estimated, optical absorption spectroscopy is also used to support this estimation. The greatest power factor was shown to be at 22 % oxidation. This is after an exposure time of 10 minutes to TDAE.

This change in oxidation level has also been looked at by changing the reducing agent. It was proposed that using TDAE was impractical from a commercial point of view.[40] Samples were produced by spin coating and then removed from the substrate in strips. The samples were then soaked in EG for around 20 minutes after this step they were washed with ethanol and the reducing agent applied to the surface of the polymer for 10 minutes. Organic reducing agents were used as received and reducing salts were made into a 10 wt% solution. The soaking in EG is to allow de-doping as described previously.[6] These steps were reversed in some samples to see if this had an effect. Figure 6 shows the Seebeck coefficient measured for the samples along with the redox potential.

Entry	Reducing agent	Redox potential E° [V/SHE]	EG-dipping	Seebeck coefficient [μV K^{-1}]
1	None	N/A	[a]	18
2	$Na_2S_2O_3$	−0.57	[a]	59
3	TDAE	−0.71[c]	[a]	43
4	Na_2SO_3	−0.93	[a]	70
5	Hydrazine	−1.16	[a]	92
6	$NaBH_4$	−1.24	[a]	104
7	$Na_2S_2O_3$	−0.57	[b]	37
8	TDAE	−0.71[c]	[b]	161
9	Na_2SO_3	−0.93	[b]	39
10	Hydrazine	−1.16	[b]	153
11	$NaBH_4$	−1.24	[b]	53

[a] EG dipping performed after the reduction step. [b] EG dipping performed before the reduction step. [c] Electrochemical potential measured in CH$_3$CN vs. the standard calomel electrode.

Figure 6 Thermoelectric power enhancement of PEDOT:PSS films through treatment with aqueous and organic reducing agents, reproduced from reference 37

The reduction level was estimated using ultraviolet–visible-near-infrared spectrophotometry (UV-Vis-NIR) as the absorption of the di-cation, radical cation and neutral chain differs. The di-cation absorbs in the 1250 - 2300 nm range, radical cation in the 625 -1250 nm range and neutral chain in the 450 – 750 range. By comparing the ratio of these peaks the reduction level can be estimated.[40] The reduction level was shown to increase with redox potential,

however; it is clear from figure 6 that the Seebeck coefficient does not follow this trend. These reduction levels were shown to decrease after reduction had finished, this phenomena was seen if the sample was left in air or encapsulated. This levelled out at around 40 $\mu V\,K^{-1}$, around double of that produced for standard PEDOT:PSS.

It is clear that 10 minutes was chosen to match that of reduction using TDAE on PEDOT:Tos, however using just this time for all reductions does not allow peak reduction level to be found in each sample. Furthermore the application of TDAE is different than that used previously, here with direct contact of liquid TDAE, previously with only TDAE vapour in contact. This study also only comments on Seebeck coefficient, this is likely due to the difficulty to get thermal conductivity measurements. Thermal and electrical conductivity is crucial to see whether use of any of these reducing agents would effect this and therefor the thermoelectric figure of merit.

It is common practice to add 5 wt% EG or DMSO, this is to increase the conductivity by allowing grains to merge.[24, 38] This helps the conductivity by removing the number of nonconductive shells and decreasing average electron hopping distance. These are not the only additives to have this effect.[41] Anionic surfactants have been shown to have the same effect as well as approving the wettability of inks. This allows for better print quality. Sodium dodecyl sulphate (SDS) was chosen for these studies, and a 30 wt% solution was added to a Clevios PH510. The PEDOT:PSS and surfactant solution were mixed at a ratio of 20:1 (v/v). Thin films were then made via spin coating. With addition of the SDS over a control, which was treated with 20:1 (v/v) of water, S was shown to decrease from 17.8 $\mu V\,K^{-1}$ to 13.1 $\mu V\,K^{-1}$. However, σ, increased from 0.61 $S\,cm^{-1}$ to 70 $S\,cm^{-1}$ causing the power factor to increase by a factor of ≈ 60.

2.4   Processing methods

As described above the main focus within processing methods is printing, by ensuring a material is printable in some cases the output of the device can be compromised. Table 4 shows a comparison of devices made by different methods.

Table 4 shows the versatility of printing methods with many different flexible devices being made. The devices have also been made by varying the number of thermocouples ranging from 4 to 1985. It is difficult to compare the performance of these devices as they are often

very different from each other in size, thickness, temperature difference and the intended orientation of the thermal gradient.

Many of these devices were printed on Kapton. This is done due to its high temperature and chemical resistance, flexibility and as it offers a flat surface. This enables a good reproducibility of devices, however printing onto fabrics is not like this. Reproducible screen printing has successfully been achieved on a flexible glass fabric.[10] This was done with Bi_2Te_3 and Sb_2Te_3 mixed with epoxy. Glass fabric was used to the high annealing temperatures (530 ^oC), however, it is unclear about use of this fabric for clothing due to weight and comfort. Flexible printed copper electrodes were used to complete the device. To safely incorporate the device PDMS has been used, this assists with the use of flexible copper, however, this would likely compromise use for fabrics as it makes the device bulkier.

METHODS	P-TYPE	N-TYPE	D_{FILM} /μm	R_{IN} /Ω	ΔT/K	N	V_{OC} /μV	P_{MAX} /μW	REF
SCREEN PRINTING	Sb_2Te_3 /epoxy	Bi_2Te_3/epoxy	500	<1	50	8	90	10.5	[10]
	PEDOT:PSS	—	1.3	138	65	576	0.18	5.5 E-5	[42]
	—	CNT composite	0.1	26	100	5	20	4	[43]
	Sb_2Te_3/PEDOT:PSS	Bi_2Te_3/PEDOT:PSS	40	145	50	7	85	12	[44]
	PEDOT:PSS	—	20	10	100	300	40	50	[44]
	Sb_2Te_3/epoxy	Bi_2Te_3/epoxy	65	800	20	4	25	0.19	[9]
	CNT/polystyrene	—	150	352	70	1985	305	66	[45]
	Sb_2Te_3/epoxy	Bi_2Te_3/epoxy	60	7200	20	8	36	0.04	[46]
INKJET PRINTING	Sb_2Te_3/epoxy	Bi_2Te_3/epoxy	500	300	30	20	25	2	[8]
	poly[Cu_x(Cu-ett)]/PVDF	poly[K_x(Ni-ett)]/PVDF	3	54	25	6	15	1	[47]
DISPENSER PRINTING	—	$Bi_2Te_{3-x}Se_x$ /epoxy	120	480	20	62	220	25	[48]
	$Bi_{0.5}Sb_{1.5}Te_3$/epoxy	—	120	800	20	60	270	21	[49]
	$Bi_{0.5}Sb_{1.5}Te_3$/epoxy	Bi/epoxy	120	100	70	10	210	130	[50]
MOLDING	$Bi_{0.5}Sb_{1.5}Te_3$/epoxy	$Bi_2Te_{3-x}Se_x$/epoxy	4000	170	25	15	35	5	[51]
	Cu(I)-ett	poly[K_x(Ni-ett)]	5000	557	60	220	1510	1000	[52]
LITHOGRAPHY	PEDOT:Tos	TTF-TCNQ	30	—	10	54	—	0.13	[36]
	Sb_2Te_3	Bi_2Te_3	0.7	2400	20	63	37	0.14	[53]
VACUUM DEPOSITION	$(Bi_{0.15}Sb_{0.85})_2Te_3$	—	200	77	34	24	130	55	[54]
	$Bi0.4Sb1.6Te3$	$Bi_2Te_{2.7}Se_{0.3}$	1	1200	130	18	600	100	[55]
	Sb_2Te_3	Bi_2Te_3	16	8300	20	10	42	5.3 E-2	[56]

Table 4 The state of the art in predominantly printable thermoelectric devices. Table in main reproduced from reference [8]

Some of the devices in table 4 were made with thousands of thermocouples. This shows that large scale production of these devices can be done. Screen printing can be achieved on a roll

to roll basis and this has been done for thermoelectric devices using silver and PEDOT:PSS. [42] The fabricated device although not made for use as wearable was flexible and could be used for mass production.

PEDOT:PSS has also been integrated into fabrics making composite materials.[57] For these PEDOT:PSS (Clevios PH1000) was drop casted onto non-woven fabrics and dried at 70 °C for 100 minutes. Further annealing at 150 °C for 30 minutes was necessary. Many composites where made with PEDOT:PSS concentrations in these materials varying from 3 to 24 wt%. The thermoelectric properties of these composite materials were then determined and the ZT was estimated to be 0.0013 for composite with 18 wt% PEDOT:PSS. These composite materials were flexible and light.

This idea of composite materials has been furthered by the creation of a PEDOT:PSS/Lycra fabric.[58] This was made by drop casting a solution of freeze dried PEDOT:PSS and spandex yarn with varying ratios from 100 % PEDOT:PSS to 100 % Lycra. The film was made by drying at 80 °C and then mechanically removed. The fabric was shown to have duel properties based upon the ratio, the optimum was found to be 90 % Lycra 10 % PEDOT:PSS. This maintained high electrical conductivity of 79 ± 5 S cm^{-1} and Seebeck coefficient of 16 ± 1 $\mu V\,K^{-1}$. The material had very similar mechanical properties to that of Lycra, although, electrical properties were found to be inversely proportional to the strain on the material.

2.5   Conclusion

Wearable thermoelectric devices are improving to a point where they could start to replace batteries in low power devices. Many of the current devices are produced by mounting commercially available thermoelectric generators onto clothing. Alongside this there is real progress with printing flexible substrates which, although mainly printed onto non wearable samples could also be printed onto fabrics. Due to the inherent flexible properties of PEDOT:PSS among other advantages over inorganic alternatives these are the future of wearable thermoelectric generators. To achieve this the thermoelectric figure of merit for PEDOT needs to be improved. This could be achieved by exchanging PSS for a different polymer. Many of the methods explained above with regards to processing methods where achieved from commercially available pastes. These are often designed for high conductivity and good printability. To achieve good printability often many additives are used to produce

the correct viscosity for the printing methods. It is unclear how these additives effect the resultant thermoelectric properties of the film thus in this research a ground up approach is being taken. Diverting from the commercially available inks will be key to improve the efficiency of the devices from the current highest figure of merit of 0.42.

Chapter 3 Experimental Detail

3.1   Introduction

The experiments have been split into 2 parts with the first involving printing techniques and analytical techniques used on commercial PEDOT:PSS ink. The information regarding this can be found in the first part of this section. Following this the direction moved towards creating an ink in a ground up fashion. Starting with EDOT followed by polymerisation in the presence of PSS and further doping with various organic solvents. This can be found in the second part of chapter 3.

3.2   Printing

A suitable procedure for PEDOT:PSS printing was found to be as follows. PEDOT:PSS (Clevios S V3) was homogenised using a DAC 150 Speedmixer for 30 seconds at 1000 RPM. 4 mL of the solution was then loaded into a 10 mL plastic syringe barrel. A 25 Gauge tip was added. The syringe was then attached to a custom dispenser printer shown in figure 7. The vacuum pressure was set to be 40 kPa, X and Y resolution was set to be 0.4 mm at a dispense time of 10 ms and dispense pressure of 420 kPa. The tip was primed by dispensing at the dispense pressure and time repetitively until the tip had dispensed the PEDOT:PSS twice. The tip was set to be 300 μm from the surface, which was achieved by manually lowering the tip until contact is made and then raising. The PEDOT:PSS was then printed onto a pre-weighed Kapton or alumina ceramic substrate. When Kapton was used it was necessary for it to be taut on the stage to ensure a constant distance between sample and syringe. The samples were then cured in an oven at 120 °C for 5 minutes. In some cases multiple layers are printed onto an already printed and uncured layer. In this case up to 8 layers were printed to ensure no spreading of the ink occurs. The subsequent layers were printed in such a way that the syringe is in contact with the already printed inks. The substrates would be then cured for a longer time, up to 20 minutes for 8 layers. These samples were then weighed again and thickness measurements taken using a micrometer. Figure 7 shows the setup of the dispenser printer.
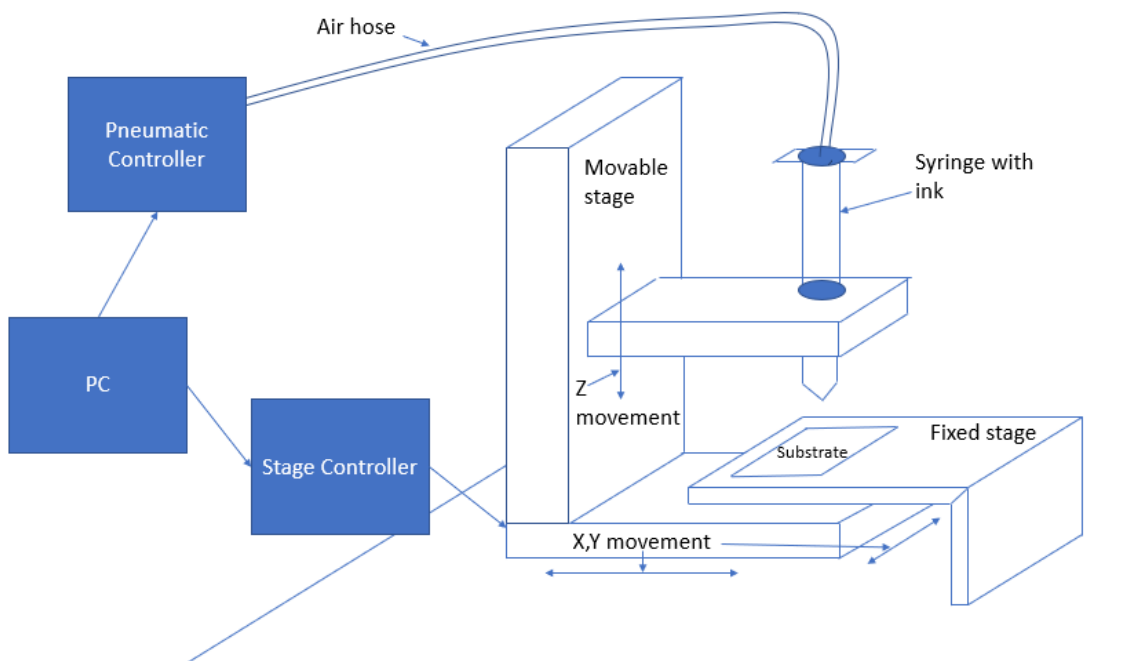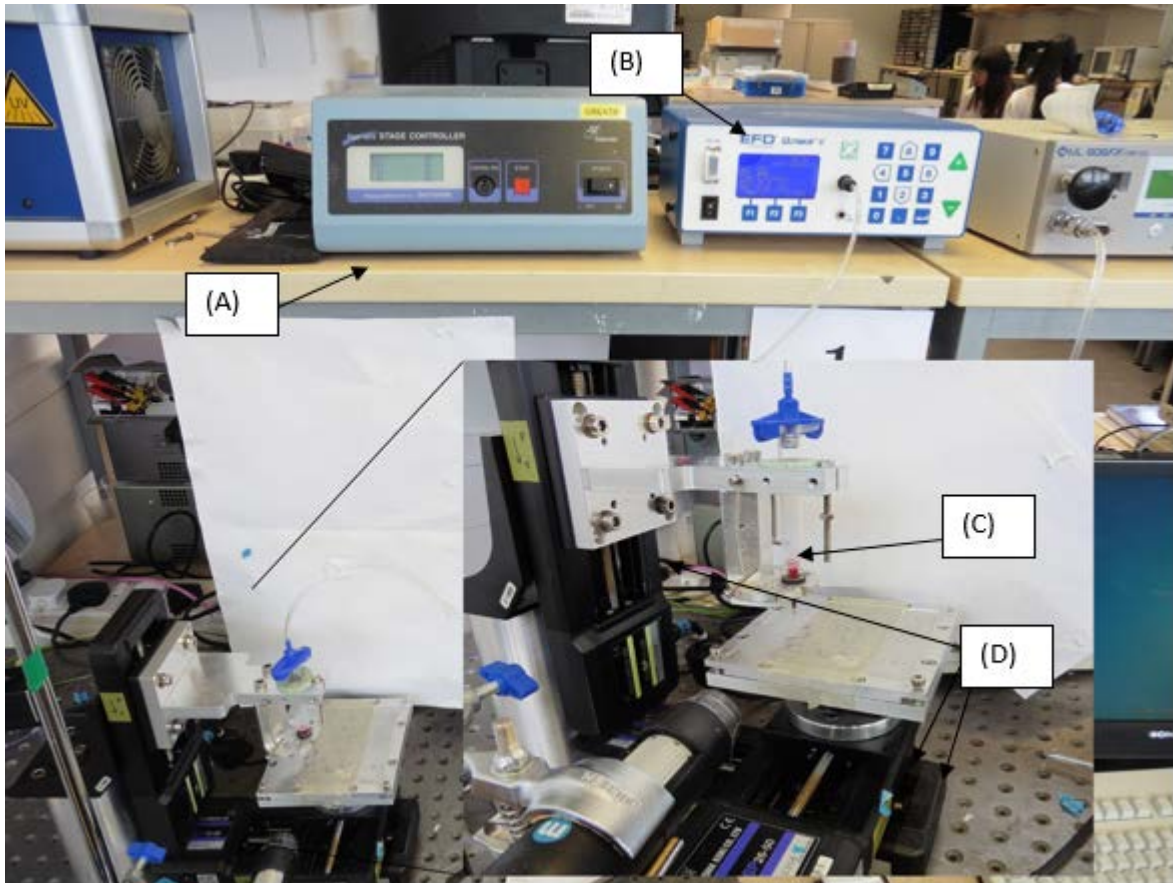
Figure 7 Photo and diagram of dispenser printer set up where labels as follows. A) stage controller B) Pneumatic controller C) Dispensing syringe D) X,Y,Z micro controllers

The above procedure was adapted for silver ink (DuPont 5000x) printing. The changes are that the dispense time was 12 ms, the dispense pressure was 410 kPa, and cure time was 9 minutes for 1 layer. Due to the use and properties of the silver ink only 1 layer was ever needed. The silver ink was used in production of devices.

3.3   Inks

PEDOT:PSS, ratios 1:1 – 1:6 were chemically synthesised using EDOT, PSS, $Na_2S_2O_8$ and ion exchange resins. The general procedure was as follows: Initially the PSS (brown powder) was dissolved in 10 mL of ultra-pure Milli-Q water. This was stirred to dissolve, $Na_2S_2O_8$ (white powder) was then added and no visible change was observed. EDOT (yellow/brown liquid) was added and small oil droplets were formed. The reaction mixture was then stirred vigorously for 24 hours with observations taken every few hours (with the exception of overnight). Normally within 12 hours the solution had changed from colourless to dark green/blue to finally black/very dark blue. On occasion after 24 hours the black/ very dark blue solution had a small oil droplet in. This was assumed to be left over EDOT, when this was observed the reaction mixture was stirred for a further 24 hours. H^+ ion exchange resin (0.5 g) was then added and stirred for a further 24 hours, finally the OH^- ion exchange resin (0.3 g) was added and stirred for a final 24 hours. In the first few occasions of purification with ion exchange resins the pH was monitored before and during, this was to ensure that 24 hours was long enough, at the point in which the pH did not change significantly over 2 hours ~0.1 g of the respective resin was added to ensure reaction to completion, each time the pH did not change again with this addition so 24 hours with the initial mases was deemed to be enough. The final solution was then decanted into a separate sample vial, and split into 5 equal portions for addition of dopant. Table 5 shows the amounts used in the reaction mixtures.

EDOT:PSS (molar ratio)	Volume EDOT / µL	Mass PSS / g	Mass $Na_2S_2O_8$ / g	Moles EDOT / mmol	Moles PSS / mmol	Moles $Na_2S_2O_8$ / mmol
1:1	75.2	0.136	0.174	0.70	0.70	0.82
1:2	75.2	0.272	0.174	0.70	0.70	0.82
1:3	37.6	0.204	0.087	0.35	1.05	0.41
1:4	37.6	0.272	0.087	0.35	1.40	0.41
1:5	37.6	0.340	0.087	0.35	1.75	0.41
1:6	37.6	0.408	0.087	0.35	2.10	0.41

Table 5 experimental amounts used to synthesise PEDOT:PSS with varying ratios

These were then diluted down to split into 4 with concentrations of 2.0, 1.5, 1.0, and 0.5 wt% in co-solvent H_2O: DMSO (90:10). The final solutions were then dried in a vacuum oven at 50 mbar and 30, 50 and 60 °C until touch dry, producing a total of 72 samples.

3.4 Characterisation

3.4.1 Thermoelectric measurements

Room temperature Seebeck measurements of PEDOT:PSS samples were taken using a homemade Seebeck machine which shows the Seebeck voltage produced from a temperature difference. Ice was used to cool the cold probe and the hot probe is at room temperature. It is necessary for the samples to be on an electrically insulating substrate, as well as this it is significantly easier to measure samples on non-flexible substrates. The machine is calibrated against a bismuth foil. Measurements were taken by placing the sample on a stage, a crocodile clip attached on one edge of the sample and a hot probe cantilever on the other edge of the sample. On soft samples this can cause scratch damage. Errors were minimised through two methods, firstly the potential shown were stable to 2dp before a reading taken and secondly at least 10 measurements were taken for each sample. Samples which have a higher electrical conductivity produce more precise results and samples with a very low electrical conductivity were unable to be measured using this equipment. This is show by a distinctly large reading, on the scale of mV or higher as opposed to μV.

3.4.2 Electrical conductivity measurements

Initial electrical conductivity and carrier concentration were measured using a commercial system (Ecopia HMS-3000). Measurements were achieved by initially attaching the sample to a printed circuit board. This was done using copper wire and applying the smallest amount of silver ink possible directly onto the sample and then using lead free solder attaching the wires to the design on the board. These contacts were done one in each corner. The Van der Pauw method was then used, naming the contacts 1 to 4 clockwise a current I_{12} is applied; this denotes a positive current being applies into corner 1 and out of corner 2. At the same time a voltage is measured across 4 and 3, denoted V_{43}. This is achieved for all 8 possible combinations, from this 8 resistances are calculated as shown in equations 4.

$$R_{12,43} = \frac{V_{43}}{I_{12}}, \qquad R_{21,34} = \frac{V_{34}}{I_{21}}, \qquad R_{23,14} = \frac{V_{14}}{I_{23}}, \qquad R_{32,41} = \frac{V_{41}}{I_{32}},$$

Equations 4 $\qquad R_{34,21} = \frac{V_{21}}{I_{34}}, \qquad R_{43,12} = \frac{V_{12}}{I_{43}}, \qquad R_{14,32} = \frac{V_{32}}{I_{14}}, \qquad R_{41,23} = \frac{V_{23}}{I_{41}},$

From this the sheet resistance can be calculated using the Van der Pauw equation, equation 5

Equation 5 $$e^{-\frac{\pi R_A}{R_S}} + e^{-\frac{\pi R_B}{R_S}} = 1$$

Where

Equation 6 $$R_A = \frac{R_{21,34} + R_{12,43} + R_{43,12} + R_{34,21}}{4}$$

Equation 7 $$R_B = \frac{R_{32,41} + R_{23,14} + R_{14,23} + R_{41,32}}{4}$$

Then by multiplying the sheet resistance with the film thickness gives the bulk resistivity of the sample. Bulk carrier concentration is also calculated using the same equipment, this is done using the hall voltages. The calculation is automated within the provided software.

After the initial ink measurements different equipment was used to determine the electrical conductivity of the lab made ink this was an Accent HL5500PC. This equipment worked in the same way however instead of having to use solder onto a sample a simple spring probe could be used. This allowed quick succession of measurements. This was not used to repeat the

initial measurements for the commercial ink as the equipment was only available later in the project.

3.4.3   XPS

Samples can be further analysed by XPS. This is useful to determine the composition of the films and dopant level. XPS is a surface sensitive technique where high energy x-ray energy is fired at the sample in a specific point. Electrons absorb this energy and are ionised, these electrons are detected and the binding energy calculated based on the energy of the electron. Binding energies for electrons are dependent on the atom they are bound to and the chemical environment the element is in, this is crucial as the binding energy for S(2p) in a sulphonate group can be differentiated from that of S(2p) in thiophene related structures.

Chapter 4 Results and discussion

4.1 Commercial inks

4.1.1 Seebeck results

8 PEDOT:PSS samples (1 cm x 1 cm) were prepared as described above and the room temperature Seebeck coefficients were calculated using equation 1. Figure 8 shows a representative example of these samples. 10 readings were taken for each sample and then averaged. From this the Seebeck coefficient was determined to be $13.55 \pm 0.34\ \mu V\ K^{-1}$. Sample thickness was measured at 10 points along each sample and on average for 8 layers the PEDOT:PSS thickness was 12 μm.
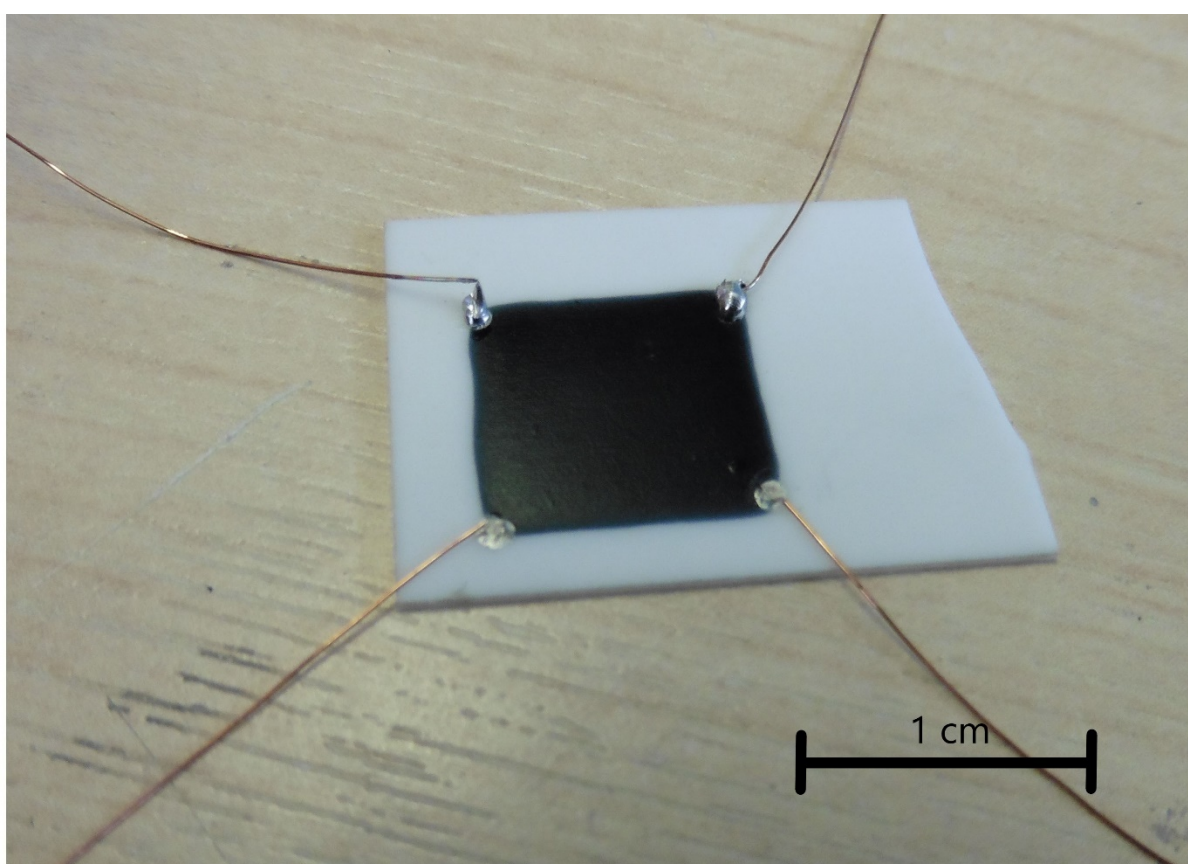

Figure 8 Example of 1 cm x 1 cm PEDOT:PSS printed on alumina substrate, thickness of PEDOT:PSS is 12 μm

4.1.2 Electrical conductivity

Attempts for electrical measurements on 7 samples were unsuccessful; this is due to the difficulty in creating an electrical connection to PEDOT:PSS. Initially a conductive epoxy was used (Circuit works cw2400). This set well however was not electrically connected to the samples. It is unclear as to why, however, this was seen in all samples in which measurement were attempted in this method (5 out of 8). For 2 other films, lead free solder was used. This

did make an electrical connection however, it was difficult to get the solder to adhere to the surface, this in large part is likely due to the melting point of solder being ≈30 °C higher than that of PEDOT. An electrical connection has been made well on an 8th PEDOT:PSS sample (1 cm x 1 cm) using silver ink (DuPont 5000x) and then curing the sample as described above. It was not necessary to print the silver, simple dipping the coper contact in the ink and then onto the corner of a sample worked fine. However this contact was very brittle. Due to the difficulties in taking the measurements only a singular measurement was taken of one sample. This sample was found to have a conductivity of 185 S cm^{-1}. This is on the scale of expected with typical literature values for optimised PEDOT:PSS being ≈ 150-2000 S cm^{-1}. Difficulties in taking the electrical conductivity measurements meant an alternative method had to be found for any further measurements. It was also decided that although the power factor could be now calculated it would be unreliable due to only a singular value for electrical conductivity being able to be measured.
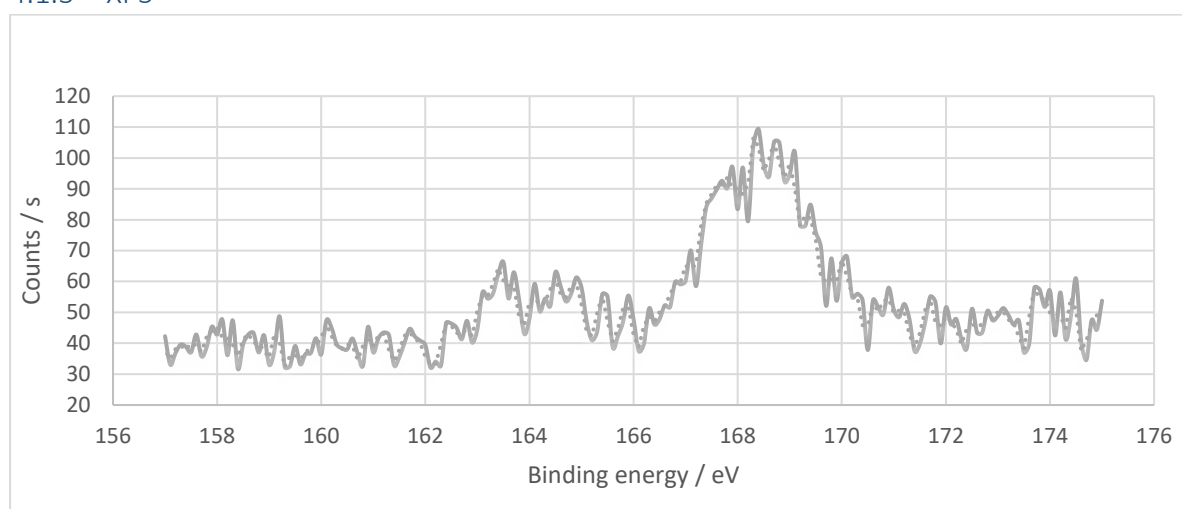
4.1.3 XPS

Figure 94 XPS analysis of PEDOT:PSS sample in the S(2p) region, peak at 168 eV corresponding to PSS and that at 164 eV corresponding to PEDOT

XPS was used on a sample to determine the PEDOT:PSS ratio. This was using a Thermo Scientific Theta Probe XPS System MC03. The main area of interest was the binding energy for S(2p), however, as well as this the O(1s) peaks were also looked at. This is because the S(2p) binding energy can be used to determine the ratio of PEDOT:PSS, the O(1s) peak was not supposed to be a focus but it was not as expected. Initially a survey scan was run from 1350- 0 eV, after this O(1s) 545 - 525 eV, C(1s) 298 - 279 eV and S(2p) 175 - 157 eV scans were achieved. Figure 9 shows the most important scan, S(2p): there is a distinct peak at 168 eV

and a less distinct peak at 164 eV. The peak at 168 eV corresponds to PSS and that at 164 eV to PEDOT. The XPS here is not as useful as it can be due to the low intensity of the peaks, and the noise level relative to these peaks. This is due to the relative low sulphur content within the samples compared to the oxygen and carbon content. The discrepancy in carbon and oxygen content is thought to be due to the various additives in the ink as provided. Looking at the data sheet it is shown that the PEDOT:PSS is a "dispersion in glycols".[59] These glycols will remain in the printed film as they are dried at 120 °C and glycols have a typical boiling point of above 150 °C dependant of which was used. Glycols can have many effects to an ink dependant on which are used. Whether their purpose is to increase printability by altering the viscosity, used as a dopant to further increase the stability of a positive charge on the PEDOT backbone (due to oxygens electronegativity) or any other reason there will undoubtably be an effect on the end properties on the material, likely in this case increasing the viscosity of the ink and the electrical conductivity. It is not explained the quantity or chain length of glycol both of which will have effects on properties, however, due to the size of the O(1s) and C(1s) peaks in figure 10 compared to the barely visible S(2p) I would suggest that short (up to 6 or 7 carbons) glycols were used in large quantities such as pentylene glycol. This is due to the relative intensity of the oxygen and carbon peaks shown in figure 10 at around a 3:1 ratio after taking into consideration the PEDOT:PSS. The carbon content could also be due to impurities in the sample. To compare the size of these peaks to what is expected, the carbon content is expected to be high as there are around 7 carbons per sulphur, however there should only be 2.5 oxygen per sulphur. Increasing the resolution of the S(2p) peaks will be key to being able to usefully use this technique for further analysis, the XPS apparatus is capable of etching the surface for depth analysis. Depth analysis is crucial to be able to fully understand the composition of the material. This is due to the surface sensitivity of XPS. XPS can typically analyse the top 5 nm of a sample, in a homogeneous sample this will show results which assist to analyse the bulk composition, however, PEDOT:PSS is not standardly homogeneous. As shown in Figure 5 (page 17) PEDOT:PSS has a grain structure with a PEDOT rich centre covered in a $\approx$ 3 nm PSS rich shell. This surface sensitivity can cause an issue when trying to determine the PEDOT:PSS ratio as the ratio refers to a bulk ratio. The samples will not typically show bulk ratio within the top 5 nm, they will be higher in PSS. To be able to get the desired results the sample would have to be homogenous.
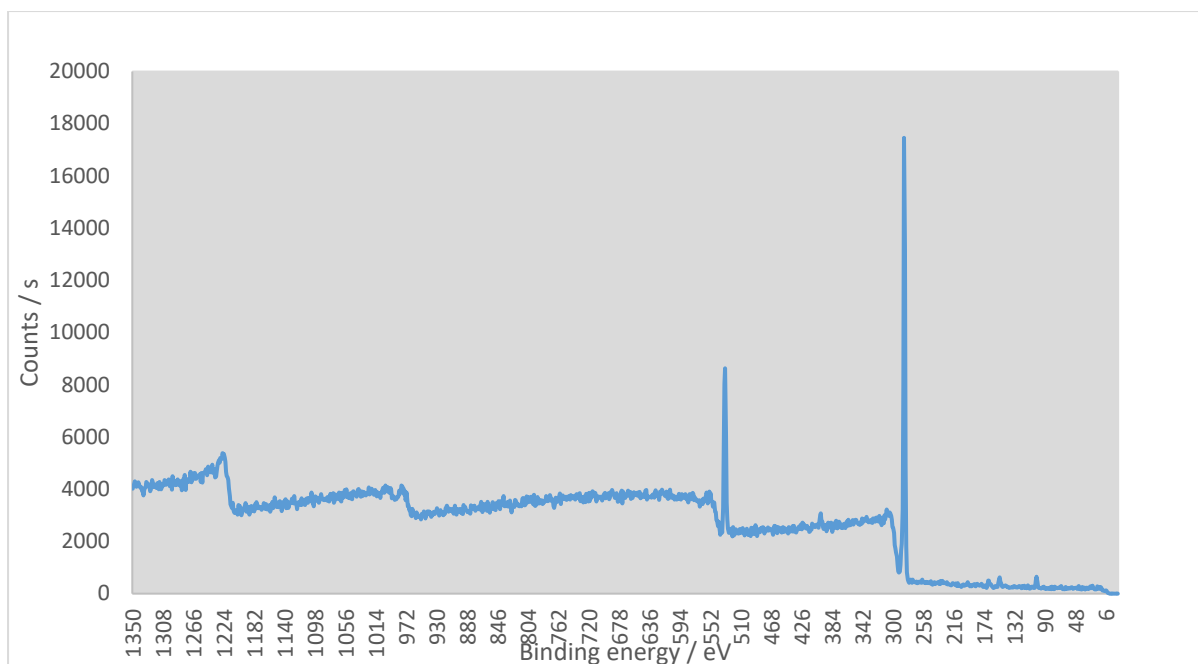
Figure 10 XPS survey scan of PEDOT:PSS, peaks at 285 eV corresponding to C(1s), 533 eV to O(1s) and almost not visible are the S(2p) peaks at 162 - 170 eV

4.1.4   Devices

Alongside these samples a test device was printed to investigate any issues when printing silver onto PEDOT:PSS on silver. The device structure was the same as shown in the roll to roll processing.[42] Figure 11 shows the flexible device printed on Kapton alongside the intended design of the device. The device has not been used to produce a voltage however an electrical connection was present through the whole sample. This has allowed some small practical considerations to be highlighted one of these being an issue with alignment. The central PEDOT:PSS layer must fully enclose it's corresponding base silver layer otherwise when the final top layer is printed the current will flow directly through the silver and miss the PEDOT:PSS, due to the silver being more conductive. This sounds like a relatively simple task however each time the sample must be removed to be cured in an oven and as the substrate is flexible ensuring it is taught and in the same place each time can pose challenges.

Top Down

Top Silver Layer

Middle PEDOT:PSS Layer
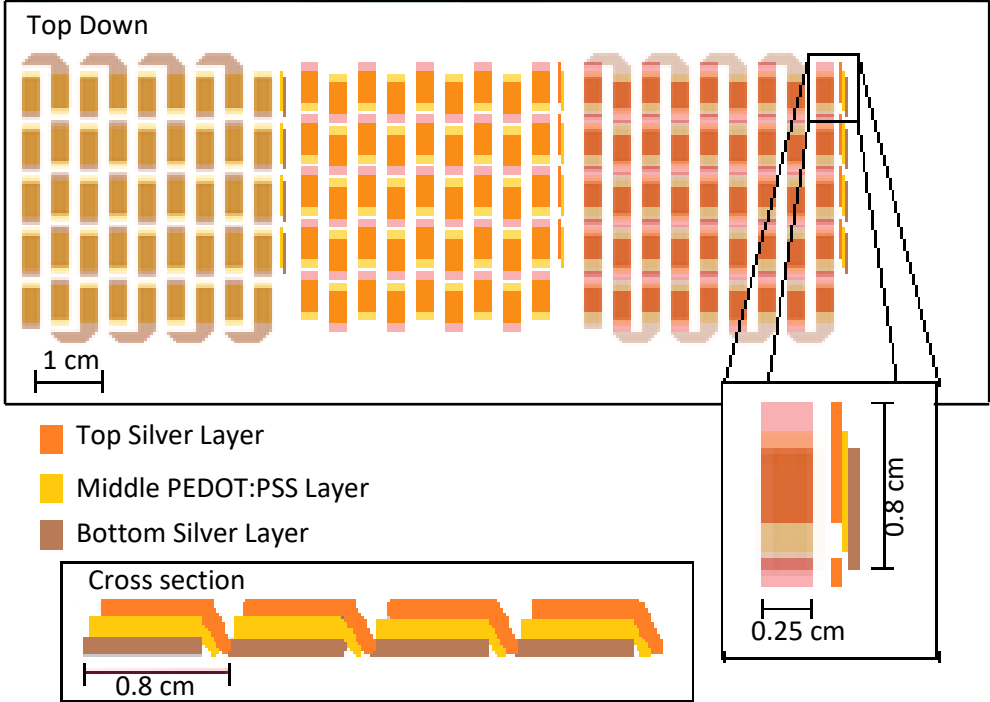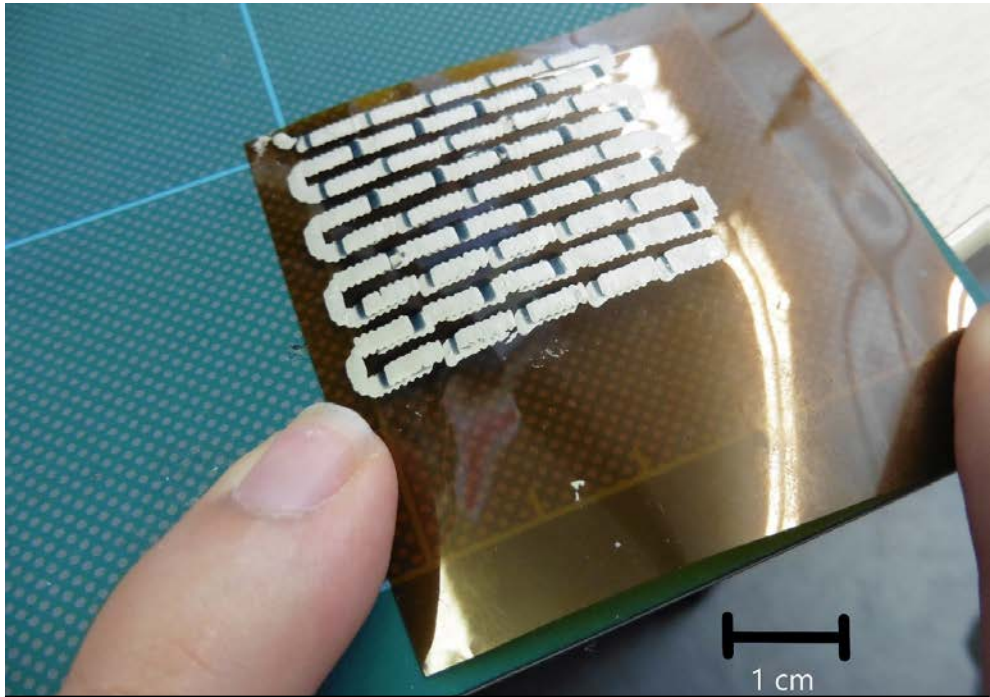
Bottom Silver Layer

Cross section

Figure 51 Image of device made by printing Silver then PEDOT:PSS then silver top electrodes. Device follows architecture shown Below the image. Set of 3 Top Down views show left. Lower and Middle layer overlap, Middle. Middle and Top layer overlap, Right. All 3 layers overlap. Bottom right shows zoomed in image to show scale of structure. Cross sectional Image shows intended overlap of Materials note. Thicknesses not shown here as variable and optimums not determined

4.2 Inks

4.2.1 Film quality

Synthesis was shown to be consistently successful. Initially films were drop casted from a mix of water then either DMSO or ethylene glycol with 10 wt% PEDOT:PSS. This produced very low quality non continuous films shown in figure 12.
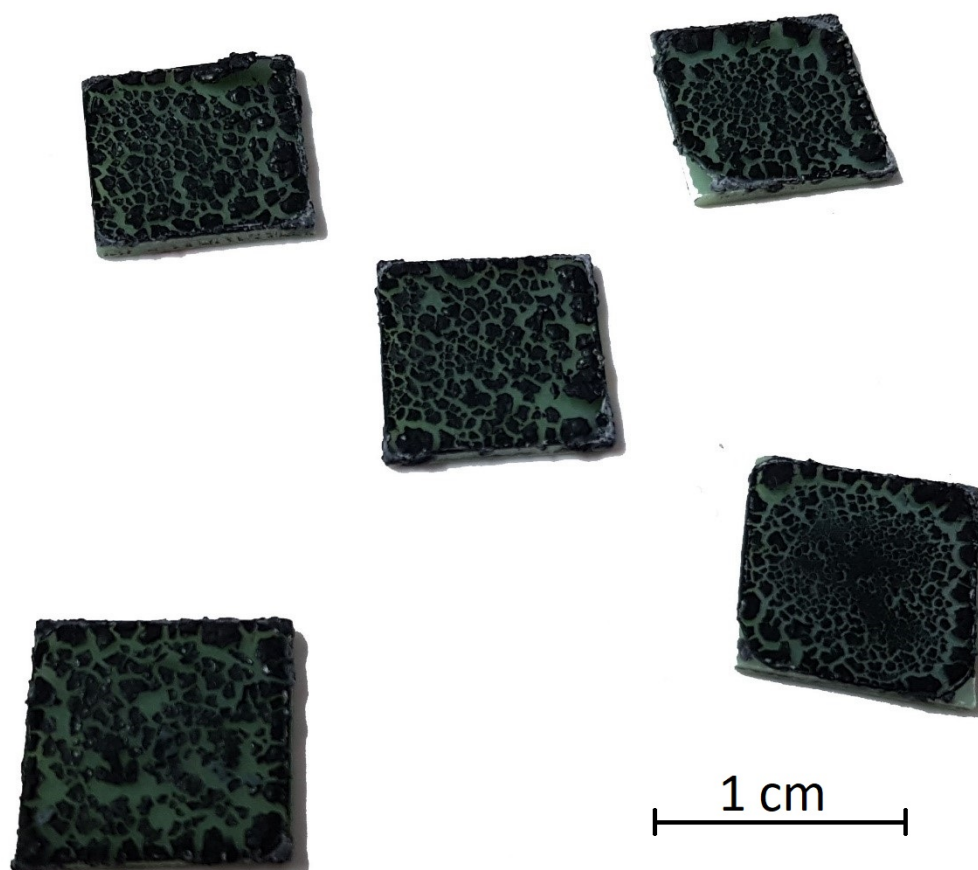

Figure 62 Drop casting PEDOT:PSS (1:1) 10 wt% in solution. Samples were dried at room temperature at low vacuum pressure. Top two and middle doped with ethylene glycol in order 5 %, 10 % and 15 %. Bottom two doped with DMSO, 5 % and 10 %

It was determined that the poor film quality was due to the solution being too high in concentration and containing non dissolved PEDOT:PSS. These cause aggregation as the water evaporated, creating mounds as opposed to a uniform film. Solutions were always homogenised before being split into portions, however then they were left for any un-dissolved PEDOT: PSS to settle to the bottom. Only the supernatant was used in future drop casts.
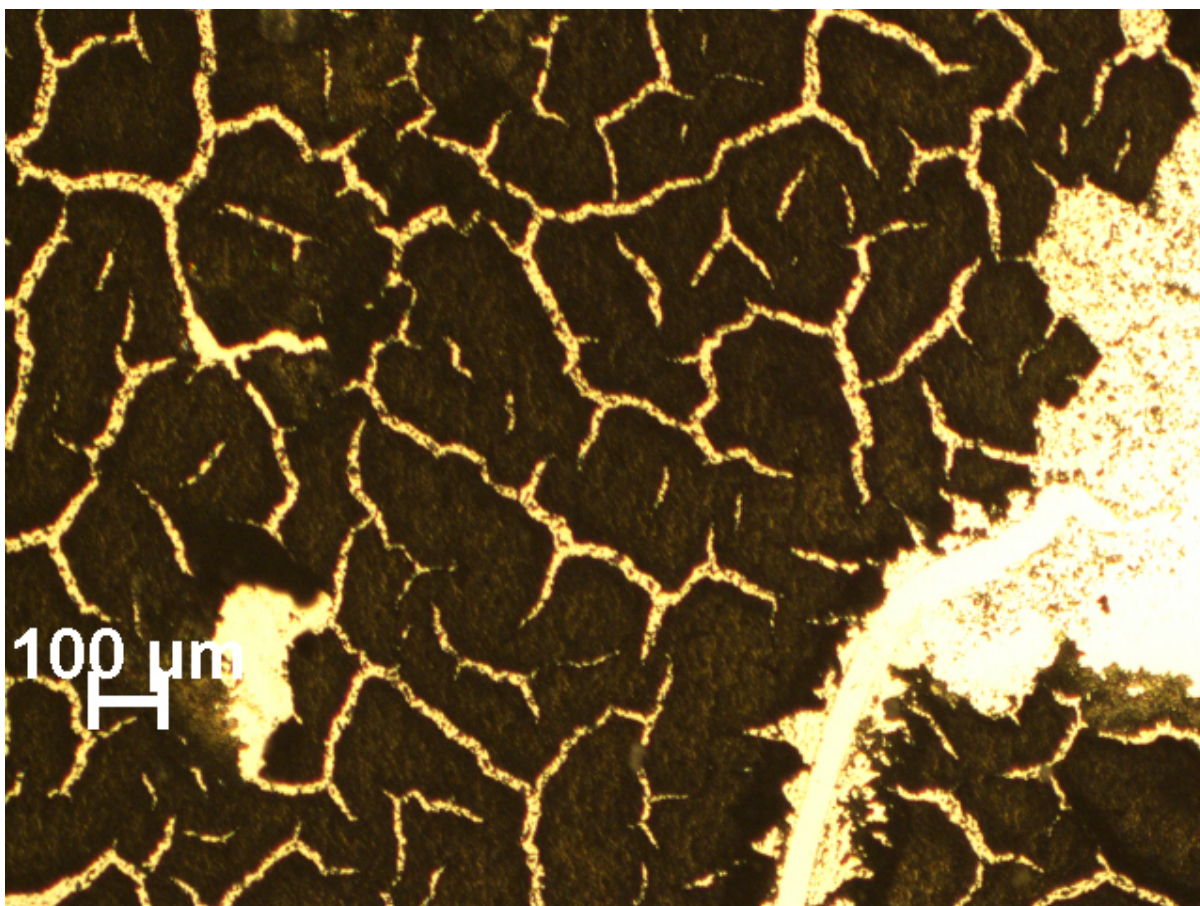
Figure 13 PEDOT:PSS drop casted on soda-lime-silica glass. PEDOT:PSS 1:1.8 10 wt% in H_2O:DMSO 90:10 pre drying. 5 x magnification.

Even just using the supernatant proved to provide low quality inconsistent films as shown in Figure 13 from a drop casted sample at 5 x magnification. At first glance before analysis under a microscope the film looks to be continuous and of good quality. However it is clear from the microscope image that there were large areas of non-continuous film. This obviously is a key component in achieving a conductive pathway across the film. Solutions were then diluted to 2.0, 1.5, 1.0, and 0.5 wt% PEDOT:PSS to determine which would produce the best film quality to be able to successfully monitor the electrical properties.

From these the 2 wt% samples were cracked especially at the lower ratios, surprisingly all temperatures produced high quality samples. 1 wt% often produced the most continuous films. As each temperature produced high quality samples this wasn't repeated but electrical measurements were achieved on these samples. Figure 14 shows an example of the new continuous films for comparison. They are more transparent in nature likely due to thickness. The black marks are believed to be crystals, visually the films from this batch often have white specks on which are removed easily by compressed gas. This may be XSO_4 (where X is a

counterion) and therefore be attributed to incomplete purification by ion exchange resin or separate contamination.
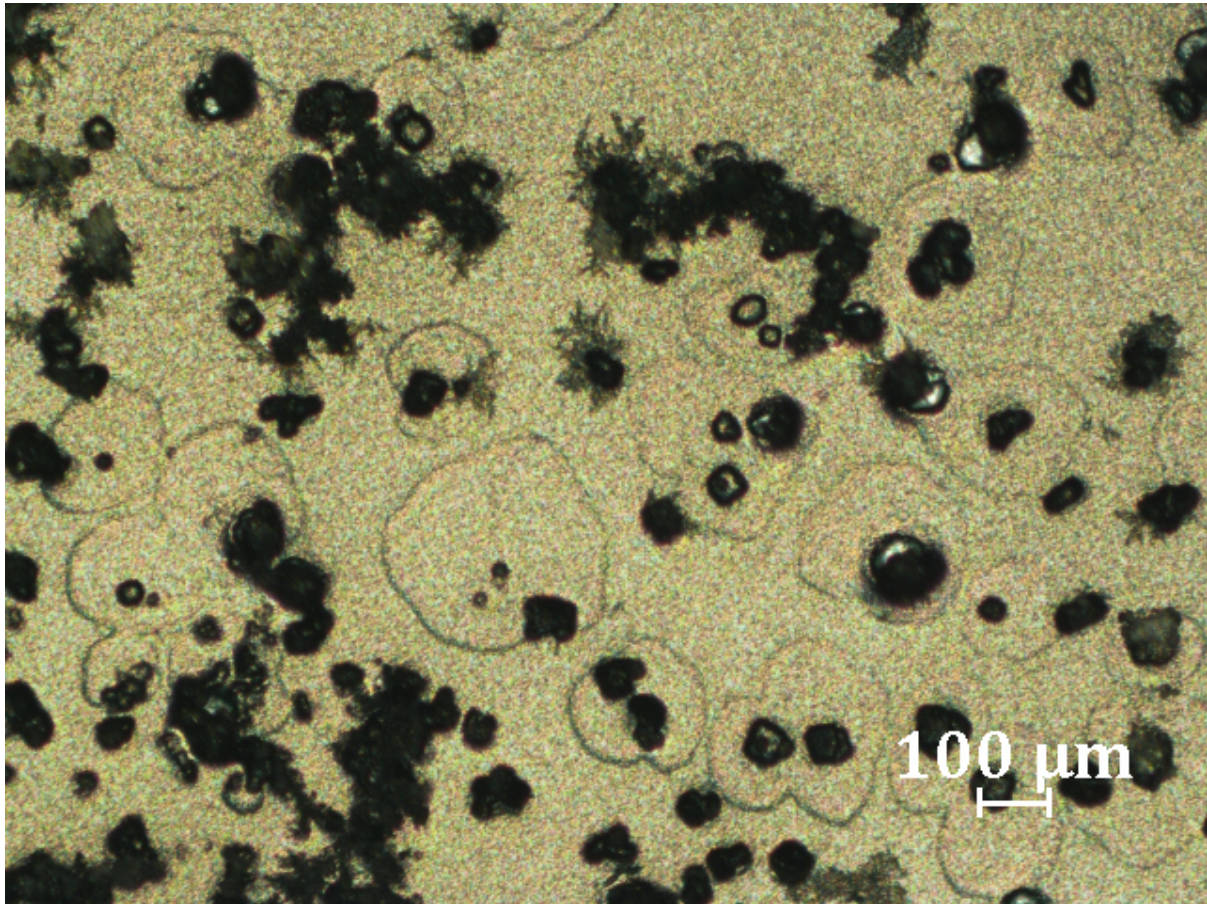

Figure 74 PEDOT:PSS drop casted on soda-lime-silica glass. PEDOT:PSS 1:4 1 wt% in H_2O:DMSO 90:10 pre drying dried at 50 mbar 60 ºC. 5 x magnification.

4.2.2   Electrical conductivity and film thickness

In this work the electrical conductivity was measured using the Van der Pauw probe method similar to that described previously, however on these the equipment used had spring loaded probes allowing a change in position easily. This allows the probes to be moved and continuity checks to be carried out to help lower contact resistances. This method also allows measurements to be taken much quicker than the previous described equipment. In this 4 metal probes where placed on the surface of the substrate. Then a current is set between 2 adjacent probes then a potential drop measured across the remaining 2 contacts. This was done in both directs for all four pairs of contacts. The sheet resistivity is calculated from this and averaged. The sheet resistivity itself is an incomparable figure relating to the substrate not the material.

To relate this to the material properties it must be multiplied by the thickness to obtain the resistivity in Ω.m as opposed to sheet resistivity in Ω.□. There are many experimental methods available to determine the thickness of a sample. In my case due to ease of access and measurement optical microscopy was chosen. Using Extended Depth of Focus (EDF) on a Nikon Eclipse LV100ND microscope with motorised focusing. Multiple images are taken at different depths and the in focus areas are then z-stacks to create 1 "all-in-focus" image. This image has the depth information imbedded and as such 3D images and Z-profiles may be created. 50/100 x magnification were chosen for this due to the decrease depth of focus with increased magnification. 100 x would have been used for all however in some cases the edge of the PEDOT:PSS was higher than the bulk film. Due to this it was ensure that the enough of the bulk film was present in the image to accurately determine the bulk film thickness as opposed to simply the thickness at the PEDOT:PSS/glass interface.
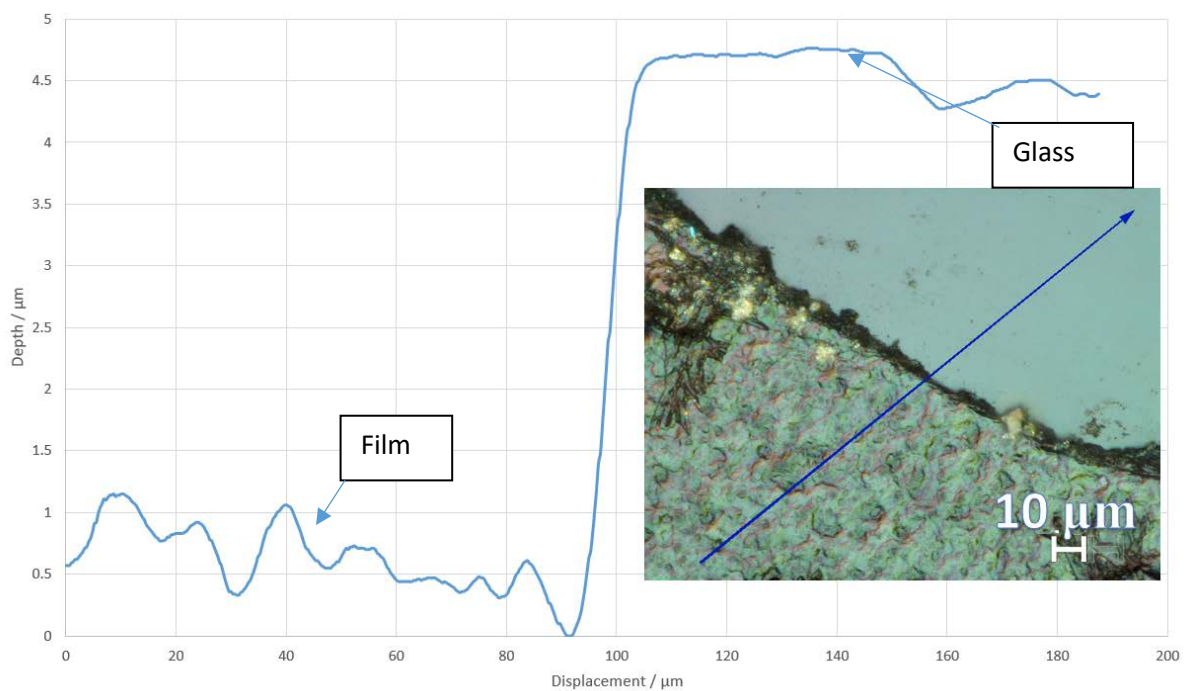
Figure 85 Step profile and associated image for PEDOT:PSS 1:5 made using EDF at 50 x magnification.

Figure 15 shows an example step profile, The 0 point is taken as the highest point found, the 2 flat sections indicate the glass and the PEDOT:PSS. The two sections are independently averaged and a 95 % confidence level taken. From this a maximum and minimum thickness is calculated as the absolute values of the differences of the furthest and closest values. Each sample had 3 values for thickness calculated at different points across the film. The 3 averages and 6 95 % confidence values were analysed with descriptive statistics giving a single value

for each sample and an error associated. These were used to calculate the sheet resistivity which was inversed to provide the sheet conductivity.
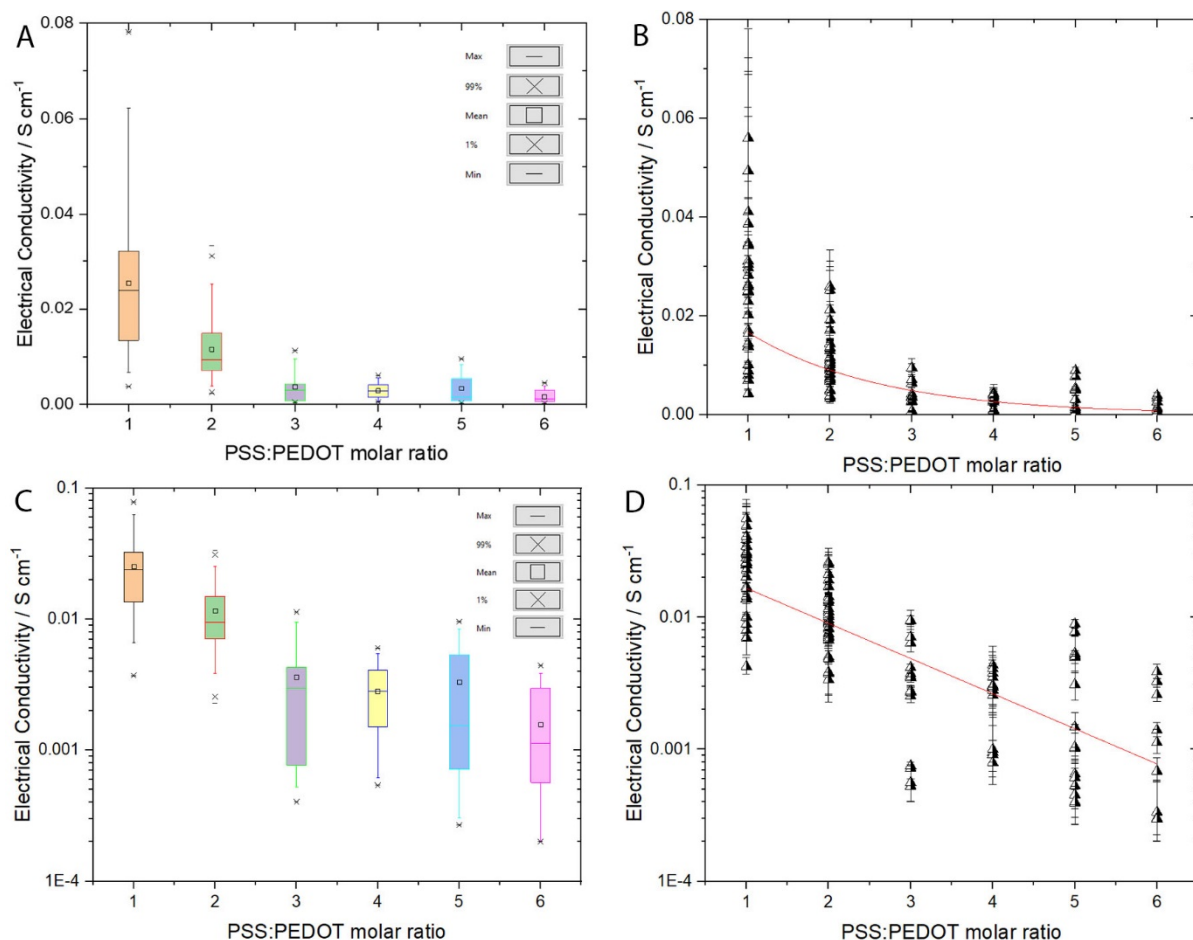

Figure 96 Electrical conductivity of PEDOT:PSS with different molar ratios, drop casted in 2 % solution with 90/10 water Ethylene Glycol Solvent. All 4 graphs have the same data with graphs C and D having a log_{10} scale on the Y axis

4.2.3 Error reducing and accounting

Figure 16 shows the relationship between the PSS/PEDOT ratio and the conductivity with either a linear or log_{10} scale on the Y axis. These were taken using the second method where spring probes were used instead of having to solder to the sample. The results reported in figure 16 are as follows, in graphs B and D each data point is a calculated conductivity from a particular sample. The data points from a particular PSS:PEDOT molar ratio are from repeat electrical conductivity measurements from 3 samples. The error reported in the error bars is due to the 3 thickness measurements from each sample. The boxplots shown in graphs A and C are an accumulation of all the data from a particular PEDOT:PSS ratio including the 95 percentiles calculated from the errors in thickness measurements. Due to the softness of the PEDOT:PSS the probes needed to be cleaned with a course material such as a sand paper

gently then before each measurement a test was done on a highly conductive material, such as a nickel foil. This was a quick test to ensure any contamination had been removed. The contact resistance is not expected to be considerably different between samples as they are all the same general material, production method and have very similar physical properties. Furthermore as the samples are soft the probes do compress the material. This compression will allow contact around the tip of the probe not only on the face edge. This helps to remove resistance from any surface issue, such as surface oxidation or surface contamination.

Samples showed some non-uniformity in appearance. This is a general problem with drop casting and drying,[16] there are many processes which occur during drying, for instance diffusion of particles towards the edge of the samples causing the "coffee ring effect". Thankfully after the initial drying condition tests these did not pose a large problem just minor non-uniformity. To mitigate this in the measurements of thickness and electrical conductivity many measurements across the sample were taken. This allowed the error to be taken into consideration from repeat measurements, this error is taken into consideration in Figure 16 showing the error bars.

There is also an error collected when calculating the thickness of the samples, as described previously the thickness is calculated through optical microscopy, using EDF. The error in the thickness value used in each calculation is gained by taking at least 3 measurement at different areas of the film, each time ensuring these are reasonable values given. For each of these as mentioned above the average of the glass height and PEDOT:PSS height are taken and a 95 % confidence limit calculated. This gives a reasonable maximum and minimum value for each reading. Once all thicknesses have been measured the averages and minimum and maximum values are all averaged and again the 95 % confidence level taken.

4.2.4 Discrepancy with literature

The electrical conductivities here are shown to be very low in comparison to literature values. This in part can be attributed to no post print processing here. As described in the literature review the expected effect of adding DMSO as achieved in these experiments is an increase in the conductivity from around 0.3 S cm^{-1} to 100+ S cm^{-1} . This increase is attributed to a change in conformation of the polymers. Figure 17 shows this expected change in conformation.

As explained before these substrates were dried with a mix solvent system, this is with 90 wt% H_2O and 10 wt% DMSO. This has been shown to increase the conductivity of PEDOT:PSS by up to 1000 x in comparison to just H_2O, this however has not happened in the samples from this project. The increased in conductivity from this mixed solvent process is connected to a change in conformation of the PEDOT:PSS from a coiled to an extended coil or linear confirmation. As described previously and shown in figure 17, PEDOT:PSS is a polymer
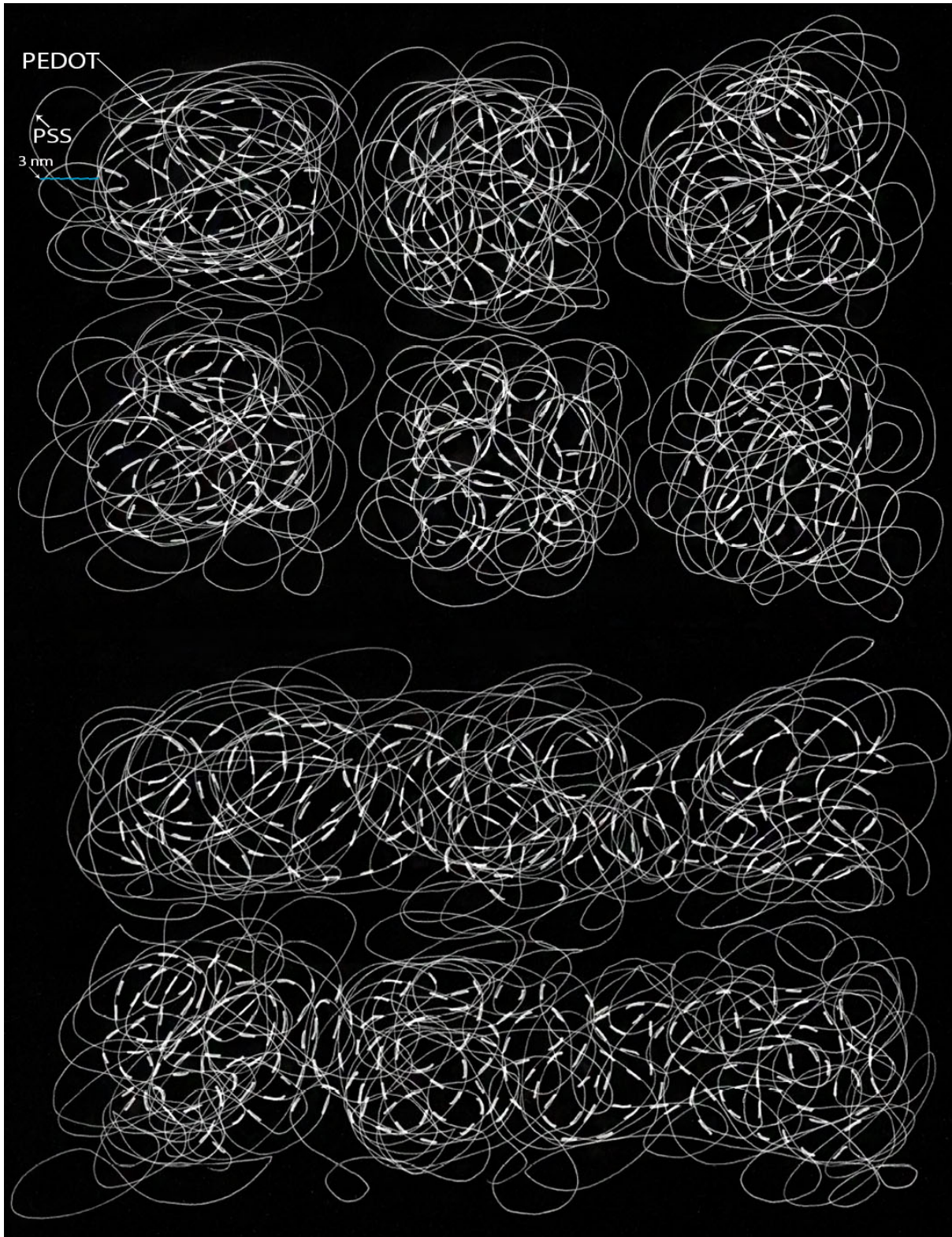
Figure 17 PEDOT:PSS drawing to represent proposed structures from literature. Top showing grain structure described in [37], bottom showing how the grains are suggested to blend with the addition of ethylene glycol

mixture of two ionomers. PSS which is non-conductive and PEDOT the conductive portion. PSS typically has a much longer length of chain and is the supportive backbone. It also charge balances the PEDOT. The issue is however that it makes these grains. Inside the grains are rich

in highly conductive hydrophobic PEDOT. The grain boundaries are almost entirely hydrophilic PSS and are thought to be around 3nm thick per grain and are what decreases the conductivity of the mixed polymer system.[60] Electrons must hop over this 6 nm gap and this, although possible, introduces a large electrical resistance into the material. Shrinking or removing this grain boundary is the target to quickly dramatically increase the conductivity of PEDOT.

The DMSO used in the experiments has been shown to remove this grain boundary entirely in areas. This is due to the hydrophobic nature of PEDOT. Introducing this high boiling point solvent has been shown to introduce a solvated PEDOT through the grain boundary decreasing the electron hopping distance between the grains to that of what is within the grains. This is shown in the second part of figure 17 in a linear fashion where side by side grains are merging however realistically they would merge in any direction.

Many studies use spin coating to make films as opposed to drop casting, this could account for some of the discrepancy in the conductivity. This is due to spin coating allowing the PEDOT molecules to align. Alignment of PEDOT can increase the intra-grain conductivity as it will allow more of the π orbitals on the aromatic systems between PEDOT molecules to align. It has been shown that for this conduction through PEDOT:PSS the distance between PEDOT molecules can have a exponential effect on the intra-grain conductivity. This alignment may account for some of the drop in conductivity. As well as this almost all samples reported in the literature were not lab made PEDOT:PSS they were commercial grade PEDOT:PSS typically with additives such as glycols mentioned previously. These will have an effect of improved electrical conductivity through assisting of merging of the grains, tailored viscosity for film making method such as printing or spin coating or perhaps an electronic influence on the energy levels of PEDOT like a dopant would.

Furthermore many of the samples are washed with other solvents including water after printing. These types of washing or changing the material post print have not been possible for my samples. This is largely due to the film quality, although good quality, consistent films were drop cased in the experiments they would lift off with any water of solvent added. This shows a clear difference in some part of the morphology of my films which I cannot find reported. This difference can also be seen between my own PEDOT:PSS and that used in the initial printing experiments shown in figure 8. This difference could come from many places however there is not enough information available to speculate which is the cause. These

include but are not limited to, impurities present in the samples, improper mixing of DMSO or chain length of PEDOT.

As described in 3.3 samples had to meet a threshold electrical conductivity to enable Seebeck voltage to be obtained, it is not clear what this exact threshold is however it is over that of 0.1 S cm^{-1}. This became apparent when Seebeck results were attempted for the in lab made samples. A typical 1x1 cm sample with a conductivity of 0.1 S/cm, higher than recorded for these samples, will have an impedance of the scale of MΩ. This was also evidenced using the digital multimeter which is used to determine potentials for the hot and cold probe as well as the sample potential. A cursory impedance measurement of samples was typically around 5 MΩ.

4.2.5 Discussing the trends

Though the DMSO has not had the desired effect there does still seem to be a trend shown in figure 16. This trend is that there is an exponential relationship between the PSS/PEDOT ratio and the electrical conductivity of samples. This is believed to be the trend despite the error in the samples. This relationship could be linked to an Arrhenius relationship shown in equation 8.

Equation 8
$$\sigma = \sigma_o e^{-\frac{E_a}{RT}}$$

Where E_a corresponds to and activation energy needed for electron transport, R is the Gas constant, T is the temperature of the sample, σ is the electrical conductivity and σ_o is a constant. This activation energy will have a dependency on proportion of conductive PEDOT to non conductive PSS. If this is linear in the range experimented in it will show as an exponential factor in σ vs PSS:PEDOT ratio. This change in activation energy is due the decreased electron hopping distance present with higher concentration of PEDOT.

From the data shown in Figure 16 an estimation of the activation energy can be taken. Assuming all samples have the same internal structure we know the expected gradient for a plot of $\ln \sigma$ vs E_a. Equation 9 shows the formula for this plot. Assuming as above that the proportion of PSS to PEDOT has a linear relationship for the region worked with here we can estimate the activation energy based on the expected gradient.

$$ln\ \sigma = -\frac{1}{RT}E_a + \ln \sigma_o$$

Equation 9

For a graph of $\ln \sigma$ vs E_a we would expect a gradient of -4.103 x10^{-4} J^{-1} mol as the samples were measured in a temperature-controlled room held at 293.15 K and the gas constant is 8.314 J.mol^{-1} K^{-1}. The plot in figure 16 D has a gradient of -0.6458, by dividing our gradient by our expected we have a conversion factor that can be used to convert our PSS/PEDOT ratio to an estimate of E$_a$. This conversion factor is 1573.97 Jmol^{-1}, Table X shows the estimated activation energy in KJmol^{-1} and eV for each sample.

PSS/PEDOT ratio	E$_a$ / KJ mol^{-1}	E$_a$ / eV
1	1.57	0.016
2	3.14	0.032
3	4.72	0.048
4	6.29	0.065
5	7.86	0.081
6	9.44	0.097

Table 6 Data showing the activation energy of electron transport with respect to the changing PSS/PEDOT ratio.

The values shown in table 6 are as described before estimates. Although they are in line with some published data there is a large error associated with this data due to the sheer spread of electrical conductivities measured.[61] The method employed here to calculate these values is also unusual, typically the electrical conductivity would be measured at varied temperature to determine each activation energy and associated error, and although this is away from the original aims of the work it would be an interesting experiment given more time. Finally again the values here assume that the dependence of the activation energy has the linear or near linear relationship associated with is with respect to PSS/PEDOT ratio. This assumption is untested however I have proposed a suggestion for the reason behind the trend seen in this data.

Another possibility for the results shown could be related to electron tunnelling. Keeping the same assumption that the change in material composition did not cause a conformational change then the changes in electrical conductivity could be caused by the tunnelling distance shrinking. The probability of electron tunnelling is exponentially inversely proportional to the distance required to tunnel, as the PSS ratio lowers the size of the grain boundaries should shrink as a higher proportion of PSS is required to charge balance the PEDOT. The electron tunnelling required is between PEDOT molecules across different grains, by lowering the size of the grain boundary the electron tunnelling probability will increase exponentially. The

exponential change seen in the overall conductivity would then show so long as the change in distance is linearly proportional to the change in electron hopping distance, this is due the electron hopping being the limiting factor in the conductivity of the overall sample.

4.3   Conclusion

In this work a method for printing devices was confirmed and shown that dispenser printing is suitable for this with simple Seebeck measurements taken. PEDOT:PSS was synthesised produced using 10 %vol DMSO as dopant to try to increase the electrical conductivity of the PEDOT:PSS the importance of film quality has been fully realised and been fixed. The sample thicknesses were successfully measured using EDF. It has been determined that the PEDOT:PSS ratio plays an important role in the electrical properties. However a 1000 X increase in electrical conductivity is necessary to compete with literature. In much of the literature this jump is attributed to dopant with solvent such as DMSO, EG or IPA. However this didn't have the same effect here. This could be related to the thickness of the samples in this research or impurities.

Chapter 5 Conclusion and further work.

5.1   Conclusion

Initial experiments were to consolidate practical techniques and conformation of material properties with respect to the literature. Seebeck measurements of commercial inks are in line with literature values and XPS results are different than expected showing a very large oxygen peak, this is believed to be down to the glycol additives.

PEDOT:PSS has been successfully synthesised and a high print quality achieved due to an initial study into best ink formulation and drying conditions. These were determined to be 1 wt% PEDOT:PSS in H_2O:DMSO 90:10 at 50 mbar and 60 ℃. Electrical conductivity has been measured for the lab produced films and are too low in currently for Seebeck voltages to be determined; the electrical conductivities measured range up to $\approx 0.6 \ S \ cm^{-1}$. This was using the Van der Pauw method and the thickness of samples determined using an optical microscope and EDF. Due to the conductivities measured it is believed the expected conformational change has not taken place. Instead the trend observed could be down to the

difference in activation energy for electron transport between samples with a difference PSS/PEDOT ratio.

There are many opportunities to adapt the thermoelectric polymer further. The ink thus far is watery in viscosity so currently unsuitable for many printing applications. However the thermoelectric performance should be improved before worrying about making it printable, as doing so is likely to lower the properties. Due to the ground up approach though all these changes can be monitored closely.

5.2   Further work

There are many directions to take this work further but of upmost importance is increasing the electrical conductivity of the lab made PEDOT:PSS to 100+ S cm^{-1}. Alternatively finding commercial additive free PEDOT:PSS to try and compare the properties to the lab made.

Now that an easily customisable ink has been made investigation into many of the methods used to increase the thermoelectric properties can be done and these can be tested with all the different compositions of PEDOT:PSS. When adapting PEDOT:PSS any initial study should be directed on causing the confirmational change and therefor hopefully achieve the jump in electrical conductivity needed. After this the focus will be on using MAI as a dopant and changing and measuring the reduction level of the samples. Etching in XPS can be useful in analysing the reduction of PSS to show whether these reductions above change the bulk composition of the films or simply the surface. If simply the surface then it may be necessary to investigate reduction before printing while the polymers are in solution form.

PEDOT derivatives will then be selected, synthesised and tested for their thermoelectric properties. The highest performing P-type molecules and a suitable metal, likely silver ink, will then be selected and a printable device made from them.

References

1.   Administration, U.S.E.I., International Energy Outlook 2016. 2016
2.   Forman, C., et al., Estimating the global waste heat potential. Renewable and Sustainable Energy Reviews, 2016. 57: p. 1568-1579.
3.   Goldsmid, H.J., Introduction to thermoelectricity. Vol. 2. 2010: Springer.
4.   C.Cullen. Thermoelectricpowergen. 2007 30/06/2017]; Available from: https://en.wikipedia.org/wiki/File:ThermoelectricPowerGen.jpg.
5.   Tritt, T.M. and D. Weston, Measurement techniques and considerations for determining thermal conductivity of bulk materials, in Thermal Conductivity. 2004, Springer. p. 187-203.
6.   Kim, G.H., et al., Engineered doping of organic semiconductors for enhanced thermoelectric efficiency. Nat Mater, 2013. 12(8): p. 719-23.
7.   Weathers, A., et al., Significant electronic thermal transport in the conducting polymer poly(3,4-ethylenedioxythiophene). Adv Mater, 2015. 27(12): p. 2101-6.
8.   Bahk, J.-H., et al., Flexible thermoelectric materials and device optimization for wearable energy harvesting. J. Mater. Chem. C, 2015. 3(40): p. 10362-10374.
9.   Cao, Z., et al., Screen Printable Flexible BiTe–SbTe-Based Composite Thermoelectric Materials on Textiles for Wearable Applications. IEEE Transactions on Electron Devices, 2016. 63(10): p. 4024-4030.
10.   Kim, S.J., J.H. We, and B.J. Cho, A wearable thermoelectric generator fabricated on a glass fabric. Energy & Environmental Science, 2014. 7(6): p. 1959.
11.   Tchounwou, P.B., et al., Heavy metal toxicity and the environment, in Molecular, clinical and environmental toxicology. 2012, Springer. p. 133-164.
12.   Andrei, V., et al., Size Dependence of Electrical Conductivity and Thermoelectric Enhancements in Spin-Coated PEDOT: PSS Single and Multiple Layers. Advanced Electronic Materials, 2017. 3(2).
13.   Luo, J., et al., Enhancement of the thermoelectric properties of PEDOT: PSS thin films by post-treatment. Journal of Materials Chemistry A, 2013. 1(26): p. 7576-7583.
14.   Zhang, S., et al., Enhancement of the thermoelectric properties of PEDOT:PSS via one-step treatment with cosolvents or their solutions of organic salts. Journal of Materials Chemistry A, 2018. 6(16): p. 7080-7087.
15.   Nardes, A.M., et al., Microscopic understanding of the anisotropic conductivity of PEDOT: PSS thin films. Advanced Materials, 2007. 19(9): p. 1196-1200.
16.   Orrill, M. and S. LeBlanc, Printed thermoelectric materials and devices: Fabrication techniques, advantages, and challenges. Journal of Applied Polymer Science, 2017. 134(3).
17.   Jang, D., D. Kim, and J. Moon, Influence of fluid physical properties on ink-jet printability. Langmuir, 2009. 25(5): p. 2629-2635.
18.   Basaran, O.A., H. Gao, and P.P. Bhat, Nonstandard inkjets. Annual Review of Fluid Mechanics, 2013. 45: p. 85-113.
19.   Krebs, F.C., et al., A complete process for production of flexible large area polymer solar cells entirely using screen printing—first public demonstration. Solar Energy Materials and Solar Cells, 2009. 93(4): p. 422-441.
20.   Sondergaard, R., et al., Energy Sci. Eng. 2013, 1, 81. Wiley Online Library| CAS| Web of Science® Times Cited.
21.   Piqué, A. and D.B. Chrisey, Direct-write technologies for rapid prototyping applications: sensors, electronics, and integrated power sources. 2001: Academic Press.
22.   Lewis, J.A., Direct ink writing of 3D functional materials. Advanced Functional Materials, 2006. 16(17): p. 2193-2204.
23.   Horii, T., et al., Synthesis and Characterization of Highly Conductive PEDOT/PSS Colloidal Gels. Transactions of the Materials Research Society of Japan, 2012. 37(4): p. 515-518.
24.   Elschner, A., et al., PEDOT. Principles and Applications of an Intrinsically Conductive Polymer, 2011.

25. Leonov, V. and R.J. Vullers, Wearable electronics self-powered by using human body heat: The state of the art and the perspective. Journal of Renewable and Sustainable Energy, 2009. 1(6): p. 062701.

26. Leonov, V., Thermoelectric energy harvesting of human body heat for wearable sensors. IEEE Sensors Journal, 2013. 13(6): p. 2284-2291.

27. Leonov, V., Thermoelectric energy harvester on the heated human machine. Journal of Micromechanics and Microengineering, 2011. 21(12): p. 125013.

28. Van Bavel, M., et al., Wearable battery-free wireless 2-channel EEG systems powerd by energy scavengers. Sensors & Transducers Journal, 2008. 94(7): p. 103-115.

29. Du, Y., et al., Thermoelectric fabrics: toward power generating clothing. Scientific reports, 2015. 5.

30. Francioso, L., et al., Flexible thermoelectric generator for ambient assisted living wearable biometric sensors. Journal of Power Sources, 2011. 196(6): p. 3239-3243.

31. Naab, B.D., et al., Mechanistic study on the solution-phase n-doping of 1,3-dimethyl-2-aryl-2,3-dihydro-1H-benzoimidazole derivatives. (1520-5126 (Electronic)).

32. Cowen, L.M., et al., Review—Organic Materials for Thermoelectric Energy Generation. ECS Journal of Solid State Science and Technology, 2017. 6(3): p. N3080-N3088.

33. Serov, A.Y., Z.-Y. Ong, and E. Pop, Effect of grain boundaries on thermal transport in graphene. Applied Physics Letters, 2013. 102(3): p. 033104.

34. Carnie, M.J., et al., A one-step low temperature processing route for organolead halide perovskite solar cells. Chemical communications, 2013. 49(72): p. 7893-7895.

35. Li, X., et al., Poly (3, 4-ethylenedioxythiophene)/graphene/carbon nanotube ternary composites with improved thermoelectric performance. Organic Electronics, 2016. 38: p. 200-204.

36. Bubnova, O., et al., Optimization of the thermoelectric figure of merit in the conducting polymer poly(3,4-ethylenedioxythiophene). Nat Mater, 2011. 10(6): p. 429-33.

37. Lang, U., et al., Microscopical investigations of PEDOT: PSS thin films. Advanced Functional Materials, 2009. 19(8): p. 1215-1220.

38. Thomas, J.P., et al., High-efficiency hybrid solar cells by nanostructural modification in PEDOT: PSS with co-solvent addition. Journal of Materials Chemistry A, 2014. 2(7): p. 2383-2389.

39. Fan, Z., et al., Higher PEDOT molecular weight giving rise to Higher thermoelectric property of PEDOT: PSS: a comparative study of Clevios P and Clevios PH1000. ACS applied materials & interfaces, 2017. 9(13): p. 11732-11738.

40. Massonnet, N., et al., Improvement of the Seebeck coefficient of PEDOT: PSS by chemical reduction combined with a novel method for its transfer using free-standing thin films. Journal of Materials Chemistry C, 2014. 2(7): p. 1278-1283.

41. Kishi, N., et al., Enhancement of thermoelectric properties of PEDOT: PSS thin films by addition of anionic surfactants. Journal of Materials Science: Materials in Electronics, 2018. 29(5): p. 4030-4034.

42. Søndergaard, R.R., et al., Practical evaluation of organic polymer thermoelectrics by large-area R2R processing on flexible substrates. Energy Science & Engineering, 2013. 1(2): p. 81-88.

43. Toshima, N., et al., Novel Hybrid Organic Thermoelectric Materials: Three-Component Hybrid Films Consisting of a Nanoparticle Polymer Complex, Carbon Nanotubes, and Vinyl Polymer. Advanced Materials, 2015. 27(13): p. 2246-2251.

44. Wei, Q., et al., Polymer thermoelectric modules screen-printed on paper. Rsc Advances, 2014. 4(54): p. 28802-28806.

45. Suemori, K., S. Hoshino, and T. Kamata, Flexible and lightweight thermoelectric generators composed of carbon nanotube–polystyrene composites printed on film substrate. Applied Physics Letters, 2013. 103(15): p. 153902.

46. Cao, Z., et al. Flexible screen printed thick film thermoelectric generator with reduced material resistivity. in Journal of Physics: Conference Series. 2014. IOP Publishing.

47. Jiao, F., et al., Inkjet-printed flexible organic thin-film thermoelectric devices based on p-and n-type poly (metal 1, 1, 2, 2-ethenetetrathiolate) s/polymer composites through ball-milling. Phil. Trans. R. Soc. A, 2014. 372(2013): p. 20130008.

48. Madan, D., et al., Enhanced performance of dispenser printed MA n-type Bi2Te3 composite thermoelectric generators. ACS applied materials & interfaces, 2012. 4(11): p. 6117-6124.

49. Madan, D., et al., High-performance dispenser printed MA p-type Bi0. 5Sb1. 5Te3 flexible thermoelectric generators for powering wireless sensor networks. ACS applied materials & interfaces, 2013. 5(22): p. 11872-11876.

50. Madan, D., et al., Dispenser printed circular thermoelectric devices using Bi and Bi0. 5Sb1. 5Te3. Applied Physics Letters, 2014. 104(1): p. 013902.

51. Jo, S., et al., Flexible thermoelectric generator for human body heat energy harvesting. Electronics letters, 2012. 48(16): p. 1015-1017.

52. Sheng, P., et al., A novel cuprous ethylenetetrathiolate coordination polymer: Structure characterization, thermoelectric property optimization and a bulk thermogenerator demonstration. Synthetic Metals, 2014. 193: p. 1-7.

53. Sevilla, G.A.T., et al., Flexible and Semi-Transparent Thermoelectric Energy Harvesters from Low Cost Bulk Silicon (100). Small, 2013. 9(23): p. 3916-3921.

54. Baba, S., et al., Formation and characterization of polyethylene terephthalate-based (Bi 0.15 Sb 0.85) 2 Te 3 thermoelectric modules with CoSb 3 adhesion layer by aerosol deposition. Journal of Alloys and Compounds, 2014. 589: p. 56-60.

55. Kato, K., et al., Fabrication of a Flexible Bismuth Telluride Power Generation Module Using Microporous Polyimide Films as Substrates. Journal of Electronic Materials, 2014. 43(6): p. 1733.

56. Mizoshiri, M., M. Mikami, and K. Ozaki, p-Type Sb2Te3 and n-Type Bi2Te3 films for thermoelectric modules deposited by thermally assisted sputtering method. Japanese Journal of Applied Physics, 2013. 52(6S): p. 06GL07.

57. Kirihara, K., et al., Thermoelectric power generation using nonwoven fabric module impregnated with conducting polymer PEDOT: PSS. Synthetic Metals, 2017. 225: p. 41-48.

58. Taroni, P.J., et al., Toward Stretchable Self-Powered Sensors Based on the Thermoelectric Response of PEDOT: PSS/Polyurethane Blends. Advanced Functional Materials, 2018. 28(15): p. 1704285.

59. Heraeus Deutschland GmbH & Co. KG Leverkusen, CLEVIOS™ S V 3 technical data sheet. Number 81075966 Issue 2016-05-03

60. Elschner, A., Kirchmeyer, S., Lovenich, W., Merker, U. and Reuter, K., 2010. PEDOT: principles and applications of an intrinsically conductive polymer. CRC press.

61. Züfle, S., Altazin, S., Hofmann, A., Jäger, L., Neukom, M.T., Brütting, W. and Ruhstaller, B., 2017. Determination of charge transport activation energy and injection barrier in organic semiconductor devices. Journal of Applied Physics, 122(11), p.115502.